Journal of Food Composition and Analysis 132 (2024) 106310

Contents lists available at ScienceDirect

Journal of Food Composition and Analysis

journal homepage: www.elsevier.com/locate/jfca

Morphology, processing attributes, fatty acid, and amino acid composition in cooked leg meat and raw hepatopancreas of juvenile male red king crab (*Paralithodes camtschaticus*) after 12 months of live holding

Grete Lorentzen [a,*], Tor Andreas Samuelsen [b], Anette Hustad [a], Tina Thesslund [a], Federico Lian [a], Bjørn Tore Rotabakk [c], Dagbjørn Skipnes [c], Sten I. Siikavuopio [a]

[a] Nofima AS, Muninbakken 9-13 Breivika, P.O. Box 6122, Tromsø NO-9291, Norway
[b] Nofima, P.O. Box 1425 Oasen, Bergen NO-5844, Norway
[c] Nofima, P.O. Box 8034, Stavanger NO-4068, Norway

ARTICLE INFO

Keywords:
Juvenile red king crab
Dry feed
Shrimps
Molting, processing
Cooked leg meat quality

ABSTRACT

This study investigated how diet composition (DC) (i.e., raw shrimp or dry feed alone and combinations thereof) affected the morphology, processing attributes, fatty acid (FA)- and amino acid (AA) composition in cooked leg meat and raw hepatopancreas of juvenile red king crabs (RKCs). After 12 months, the crab weight nearly doubled, and the average mortality was 10%. The DC influenced the attributes of the cooked leg meat and the raw hepatopancreas. In addition, crumbling the dry feed led to reduced nutritive conditions, especially in the 80 and 100% dry feeding groups. In the leg meat, the main FA components were PUFA, MUFA, and SFA in descending order, while for the raw hepatopancreas, the corresponding order was MUFA, PUFA, and SFA. Minor AA variations across the groups were observed in the cooked leg meat and raw hepatopancreas. A PCA revealed a grouping of selected morphological-, processing attributes, and FAs according to the 20 and 100% dry feed groups. This study did not explore the specific feed intake. Hence, whether the results reflect the DC, a lower feed intake due to the crumbling, or a combination is unknown. Overall, the results show positive prospects for live holding of juvenile RKCs.

1. Introduction

The red king crab (RKC) *Paralithodes camtschaticus* (Tilesius, 1815) is an exclusive and highly valued decapod species that appeals to consumers worldwide for the delicate properties of its meat. The Norwegian RKC fishery is split into two; a regulated and a non-regulated fishery. The regulated fishery is designated east of North Cape at 26°E and south of 71°30'N, while the area west of 26°E is non-regulated. In the non-regulated area (FFA), the aim is to fish as much of the RKCs as possible to limit further species migration westward (Norwegian Ministry of Fisheries and Coastal Affairs, 2007; Sundet and Hoel, 2016). Despite these measures, catches of RKCs, especially small RKCs, in the FFA continue to increase (Råfisklaget, 2024). Fishing the small RKCs (i.e., juveniles below commercial weight classes, < 800 g) often results in low profitability for the fishermen. Hence, the motivation to perform such a fishery is low.

In Norway, there is considerable interest in developing an industry for feeding juveniles or short-term live holding of adult RKCs to improve their welfare and quality (Lorentzen et al., 2018; 2023). A key factor for the success of this industry is the type of feed available, e.g., marine by-products or manufactured dry feed. The feed provides energy for growth and molting, and it should be nutritious, shelf-stable, and manufactured commercially at a reasonable price (Simon, 2009). For example, lipids are an important energy source in juvenile and larval crustaceans (Kattner et al., 2003) that are crucial in promoting growth and molting success (Wen et al., 2006). In 2006, the first successfully manufactured dry feed for maintaining survival and growth in juvenile RKC was developed (James et al., 2013; Siikavuopio et al., 2006) with feed components equivalent to the nutrition requirements for lobster (D'Abramo et al., 1997). In previous studies, shrimp, herring, blue mussels, sea urchins, capelin, backbones of saith, and lumpfish, including dry feed coated with lumpfish hydrolysate, have been used to feed both juvenile and adult RKCs (Conradi-Larsen et al., 2024; Lian et al., 2019; Lorentzen et al., 2023).

* Corresponding author.
E-mail address: grete.lorentzen@nofima.no (G. Lorentzen).

https://doi.org/10.1016/j.jfca.2024.106310
Received 3 March 2024; Received in revised form 29 April 2024; Accepted 4 May 2024
Available online 22 May 2024

In the digestive system of the RKC, the hepatopancreas is a key organ that secretes enzymes with broad specificity and high activity. It is responsible for digestion, absorption of nutrients, and storage of reserves (Cervellione et al., 2017; Dvoretsky et al., 2020). The activity of this organ is related to foraging, physiological processes associated with molting, regeneration of limbs or wounds, and reproduction (Gibson and Barker, 1979). In addition, the hepatopancreas and muscle tissue, including the abdomen of the RKCs, hold significant energy reserves. To determine the level of energy reserves, the hepatopancreas index (HSI) and the abdomen index (AI) are calculated as the ratio of the hepatopancreas and abdomen weights to the total weight of the crab, respectively (Lorentzen et al., 2023). In their natural habitat, these energy reserves are mobilized when RKC undergoes extended periods with poor availability of food items (Sacristán et al., 2017). This HSI and AI have been calculated in a variety of live holding studies of RKCs, with and without feeding (James et al., 2013; Lian et al., 2019: 2022; Lorentzen et al., 2019: 2023; Siikavuopio and James, 2013; Siikavuopio et al., 2014).

Despite concerns relating to potential allergenicity and possibly high cholesterol content, several studies have promoted the consumption of meat obtained from crustaceans, including crab species (Rosa and Nunes, 2003; Risso and Carelli, 2012). This is because the presence of essential amino acids (EAAs), high-quality proteins, and a high level of polyunsaturated fatty acids (PUFAs) (Barrento et al., 2009; Vilasoa--Martínez et al., 2007) are believed to give positive health effects, on balance. Although the amino acid composition of a range of food items has been reported (Huang et al., 2017), detailed information about the amino acid composition of food products obtained from RKCs is lacking.

This study aimed to test the effect of different diets, combining raw shrimp and dry feed, on the morphology, processing attributes, fatty acid- and amino acid composition in cooked leg meat and raw hepatopancreas in juvenile RKCs after 12 months of feeding. The raw shrimp component represents food from their natural habitat, while the dry feed represents a manufactured product that is attractive from a nutritive perspective. It is hypothesized that these two feed items, separate or in combination, can support the growth of juvenile RKCs to commercial size (>800 g). This investigation of diet compositions and their effects on growth and quality represents a novel contribution to obtaining knowledge in this field.

2. Material and method

2.1. Capture and live holding

On the 12th of May 2022, juvenile RKCs were captured in the FFA near Tromsø (~70°N, Norway). The RKCs were transported to the nearby Aquaculture Research Station (ARS) in Kårvik and placed in 6 m^3 tanks with seawater, where they were kept for observation and acclimatization until the start of the feeding experiment. The juveniles were provided with shrimp and herring during the acclimatization period.

During 14–15 June 2022, 405 vital and immature juveniles were selected for the study (Table 1). The crab weight and carapace width (CW) were registered using an electronic scale (Sartorius, Data Weighing Systems, Inc., IL, USA) and a caliper (Teco's, AJ produkter, Kløfta, Norway), respectively. Next, the juveniles were tagged in the abdomen flap using a Biomark HDX12 pit-tag (Merck Animal Health, Boise, Idaho, USA). The RKCs were then evenly distributed among 9 land-based holding tanks filled with seawater at ambient temperature. The temperatures were logged continuously (HOBO TidbiT v2 - UTBI-001, Onset®, MA, USA), while dissolved oxygen was measured weekly (YSI, ProSolo ODO/CT, Yellow Springs, OH, USA). The tanks were supplied with filtered (60 μm drum filter) and UV-treated seawater (salinity of 34‰) at 15 L/min. The light regime was regularly adjusted to match the natural photoperiod for Tromsø (70°N). The light had a color temperature of 6500 K, which is similar to natural daylight.

The juveniles were fed with raw shrimp and dry feed. The raw shrimp was purchased from Lyngen Reker AS near Tromsø. The dry feed was produced at Nofima's Feed Technology Center, part of the Aquafeed Technology Centre, using a double differential preconditioner and a co-rotating twin-screw extruder (TX-52, Wenger Manufacturing Inc., Sabetha, KS, USA). The feed was dried in a horizontal conveyor belt dryer with two drying chambers (Mitchell Dryers, CAD Works

Table 1
Morphology and processing attributes (mean ± standard deviation) of reference red king crabs before starting the feeding (Wild 2022, *n*=20), reference red king crabs for the 2023 sampling (Wild 2023, *n*=10), and red king crabs after 12 months feeding. The feeding groups include shrimps only (P0, *n*=20), 80% shrimps and 20% dry feed (P20, *n*=40), 50% shrimps and 50% dry feed (P50, *n*=40), 20% shrimps and 80% dry feed (P80, *n*=40), and 100% dry feed (P100, *n*=40).

	Wild 2022	***Wild 2023***	***Feeding groups***				
			P0	P20	P50	P80	P100
Morphology							
Weight 2022 (g)	708.00 ± 202.15*	-	385.01 ± 112.25	356.00 ± 95.80	352.00 ± 107.34	355.86 ± 102.41	371.21 ± 116.24
Weight 2023 (g)	-	673.20 ± 95.40	812.20 ± 185.59	761.10 ± 149.83	725.80 ± 228.09	790.90 ± 215.57	761.15 ± 262.15
CW 2022 (cm)	NA		8.72 ± 0.95	8.50 ± 0.93	8.41 ± 0.96	8.52 ± 0.84	8.58 ± 0.94
CW 2023 (cm)	8.6 ± 0.90	10.56 ± 0.52	11.23 ± 1.10	10.89 ± 0.79	10.68 ± 1.22	11.18 ± 1.16	11.04 ± 1.39
HSI (%)	4.99 ± 0.61	6.00 ± 0.52	4.73 ± 0.84^{abx}	5.23 ± 1.07^{ax}	4.93 ± 0.91^{abx}	4.80 ± 0.52^{abx}	4.52 ± 0.64^{bx}
MC (%)	80.16 ± 7.75	70.77 ± 4.65	$56.48 \pm 6.16^{ab\Delta}$	$58.67 \pm 9.53^{a\Delta}$	$56.88 \pm 8.86^{ab\Delta}$	$52.77 \pm 6.12^{b\Delta}$	$51.35 \pm 5.57^{b\Delta}$
AI (%)	4.46 ± 0.27	3.18 ± 0.32	$2.39 \pm 0.54^{a\Delta x}$	$2.36 \pm 0.36^{a\Delta x}$	$2.04 \pm 0.38^{b\Delta x}$	$1.70 \pm 0.20^{cd\Delta x}$	$1.51 \pm 0.23^{d\Delta x}$
Shell thickness (mm)	0.46 ± 0.03	0.48 ± 0.04	0.46 ± 0.07^{x}	0.45 ± 0.07^{x}	0.43 ± 0.08^{x}	0.43 ± 0.05^{x}	0.41 ± 0.06^{x}
BI	16.04 ± 2.78	22.06 ± 3.82	12.19 ± 3.96^{ax}	13.98 ± 3.69^{abx}	15.82 ± 3.16^{abx}	17.88 ± 10.22^{bc}	$22.00 \pm 7.98^{c\Delta}$
Processing attributes							
CY_{raw} (%)	53.66 ± 1.42	55.90 ± 0.55	54.40 ± 1.91	54.71 ± 1.57	54.23 ± 1.41	54.40 ± 1.70	54.88 ± 1.87
CY_{cooked} (%)	50.68 ± 4.62	56.75 ± 0.85	54.46 ± 2.79^{a}	53.46 ± 5.80^{a}	52.09 ± 3.15^{ax}	49.65 ± 3.87^{abx}	$46.79 \pm 4.12^{bx\Delta}$
$\Delta Cluster_{bled}$ (%)	1.60 ± 1.61	-1.82 ± 0.91	0.78 ± 2.05^{a}	$-0.98 \pm 1.88^{ab\Delta}$	-0.12 ± 2.07^{a}	$-1.82 \pm 2.54^{ab\Delta}$	$-3.60 \pm 5.15^{b\Delta}$
$\Delta Cluster_{cooked}$ (%)	-4.32 ± 6.50	1.44 ± 1.20	-0.10 ± 3.38^{a}	-2.24 ± 9.27^{ab}	-3.97 ± 4.79^{ab}	-8.53 ± 5.49^{bcx}	$-14.78 \pm 7.95^{cx\Delta}$
T_{max} (≈ 86°C)	88.48 ± 0.60	88.19 ± 0.58	87.79 ± 0.12	$87.66 \pm 0.30^{\Delta}$	$87.12 \pm 0.60^{\Delta x}$	$87.54 \pm 0.22^{\Delta}$	$87.15 \pm 0.11^{\Delta}$

* Data obtained from 20 selected juveniles slaughtered and processed before feeding study. The weight in 2022 for the P0 to P100 is obtained from 45 RKCs in each group.

NA Not analyzed

Note. Results are expressed as mean values (± standard deviation). Different superscript letters within the same row of the fed RKCs indicate significantly different mean values ($p < 0.05$, full factorial ANOVA followed by Scheffe's test). The symbol Δ and X indicates the mean values significantly different ($p < 0.05$. One-way ANOVA followed by Dunnett's test) from the mean value observed for wild crabs in 2022 and 2023, respectively.

Abbreviations. CW, carapace width; AI, abdomen index; MC, meat content; HSI, hepatosomatic index; BI, browning index of hepatopancreas; CY_{raw}, raw cluster yield; CY_{cooked}, cooked cluster yield; $\Delta Cluster_{de\text{-}bled}$, cluster weight change relative to the effect of the de-bleeding; $\Delta Cluster_{cooked}$, cluster weight change relative to the combined effect of the de-bleeding and cooking, T_{max}, the denaturation temperature during heating around 86°C.

Engineering LTD, Carlisle, UK) before the addition of oil in a Pegasus® vacuum coater (PG-60VC, Dinnissen BV, Sevenum, Netherlands). The diameter of the final feed was 5 mm, with a high bulk density that enabled it to sink in water. The disintegration properties, or feed loss in water, was measured using a water stability test (Samuelsen et al., 2022). In this test, 20 g feed was added to 500 mL distilled water and shaken at 23 °C for 120 min. Water stability was calculated as the remaining amount of feed (dry matter) not dissolved in the water. The test was run in triplicate and the water stability of the feed was 80.9 ±0.2%.

The RKCs were fed with shrimp and dry feed in five combinations: P0, P20, P50, P80, and P100, where the group number reflects the percentage of dry feed. For example, RKCs in the P0 group received 100% shrimp, the P20 group was fed with 80% shrimps and 20% dry feed and the P100 group received only dry feed. The study included two replicas, i.e., additional tanks of the feeding groups P20, P50, P80, and P100, while for group P0, a single replica tank was used. The dry feed had a dry matter (DM) content of 89.7%. The DM was correspondingly composed of 56.5% crude protein, 13.8% total ash, 19.0% crude lipid, and a gross energy of 22.3 kJ/g. The DM content of the shrimp was 27.9%, which in turn was composed of 61.4% crude protein, 12.1% total ash, 24.8% crude lipid, and a gross energy of 24.2 kJ/g. The dry feed formulation and chemical composition are given in Supplementary Tables 1 and 2.

The RKCs were fed *ad libitum*, i.e., they were offered feed in excess and fed every Monday, Wednesday, and Friday. In the P20 group, dry feed was given two feeding days in a row followed by seven feeding days with the shrimps and vice versa for the P80 group. In the P50 group, dry feed was given four feeding days in a row and shrimps the following four days. The feed volume ranged from 2.5 to 11.1 g/kg crab/day, adjusted according to the molting cycle. Specifically, appetite was reduced before molting and increased after molting and the feed volume was adjusted accordingly.

During the study, the RKCs were provided with sea sand, which has been shown to have positive effects on RKC morphology and corresponding product quality (Lorentzen et al., 2023). Dark green plastic trays with a height of 5 cm were filled with sea sand, to ~3 cm depth. The trays covered 6.2% of the tank bottom area. The sand was collected from the shoreline of Kvalsundet Strait (close to ARS). The RKCs were provided with access to the sand one week each month with newly collected sand each time.

Mortality in the tanks was assessed daily. The RKCs were defined as dead when no movement of the appendages was observed within 2 minutes.

2.2. Sampling, preparation, and processing

From 20–22 June 2023, subgroups of 10, 20, 20, 20, and 20 individuals were selected from the P0, P20, P50, P80, and P100 feeding groups, respectively. The crabs were selected randomly amongst the individuals that were not visibly injured or missed limbs. In medio June 2022 and 2023, wild RKCs were captured in Eidkjosen, near Tromsø, transported to ARS, and placed in 6 m^3 tanks with seawater. These RKCs were used as references. The selected RKCs and 20 of the wild crabs were placed in polystyrene boxes covered with a moist paper towel and gel ice (Cold Inc., Oakland, CA, USA). Next, the boxes were transported to Nofima (Tromsø) by car (30 min), stored at 1–2 °C overnight, and processed the following day as described by Lian et al. (2021) with some modifications.

Following transport, one leg on each side of the RKC was labeled using T-bar tags (Floy Tag Inc., Seattle, WA, USA). Next, the RKC was split into two clusters (i.e., three walking legs and one claw assembled in a shoulder joint), which were then placed in water at 1–2 °C for approximately 2 h to remove free body fluid (FBF). Afterwards, the clusters were removed from the water and drained for at least 15 min before weighing. The clusters were then placed in wire baskets and cooked by soaking them in water at 95 °C for 12 min, targeting a core temperature of 92 °C in the second walking legs most proximal article (*merus*). Next, the clusters were cooled in ice water with 3.5% NaCl (w/v) for a minimum of 30 min to ensure a leg core temperature below 4 °C. The clusters were then drained for at least 15 min before weighing. Next, the clusters were air-packed into plastic bags (thickness 80 μm, dimensions 220 × 600 mm, Finnvacum, Helsinki, Finland), closed with metallic clips, and stored at 4 °C in a climate chamber (BINDER, GmbH, Tuttlingen, Germany) for two days.

2.3. Analytical determinations

2.3.1. Morphology and processing attributes

The hepatosomatic index (HSI) was calculated as follows:

$$HSI = (W_H / W_{RKC}) \times 100 \quad (1)$$

where W_H and W_{RKC} are the hepatopancreas and crab weight, respectively (Lorentzen et al., 2023).

The meat content (MC) was measured by digital image analysis (ImageJ, National Institutes of Health, US) of cross-sections of the middle of the *merus* as previously described (Lorentzen et al., 2019). The MC was calculated as follows:

$$MC = (\text{Area occupied by meat} / \text{Total inner area}) \times 100 \quad (2)$$

The abdomen index (AI) was calculated as follows:

$$AI = (W_A / W_{RKC}) \times 100 \quad (3)$$

where W_A and W_{RKC} are the abdomen and crab weight, respectively (Lorentzen et al., 2023).

The shell thickness was measured in proximity to the middle of the *merus* of the second walking leg using a caliper (precision ± 0.05 mm). Residual meat and cartilage residue were removed using a scalpel and paper tissue prior to the shell thickness measurement.

The color of the hepatopancreas, measured in terms of L^* (lightness), a^* (green-red), and b^* (blue-yellow), were determined using a portable color-spectrophotometer (CM-600d, Minolta Ltd., Osaka, Japan). The browning index (BI) was calculated (Sikora et al., 2021) from the measured parameters as,

$$BI = (100\ (w - 0.31)) / 0.17, \quad (4)$$

were $w = (a^* + 1.75\ L^*) / (5.645\ L^* + a^* - 0.3012b^*)$.

From the weight of the raw RKCs and the raw clusters, raw cluster yield (CY_{raw}) is given by,

$$CY_{raw} = (W_{2CR} / W_{RKC}) \times 100, \quad (5)$$

where W_{2CR} is the sum of the weight of the right and left raw clusters from the same RKC after splitting, and W_{RKC} is the corresponding raw crab weight. Similarly, the yield of cooked clusters (CY_{cooked}) was calculated as follows:

$$CY_{cooked} = (W_{2CC} / W_{RKC}) \times 100 \quad (6)$$

where W_{2CC} is the weight of the two cooked, cooled, and drained clusters from the same RKC, and W_{RKC} is the corresponding raw crab weight.

The cluster weight relative to the effect of the bleeding step, i.e, drainage of hemolymph, was calculated as follows:

$$\Delta Cluster_{bled}\ (\%) = ((W_{CD} - W_{CR}) / W_{CR}) \times 100 \quad (7)$$

where W_{CD} is the weight of a single cluster after bleeding and drainage, and W_{CR} is the weight of the corresponding single raw cluster after splitting and drainage before bleeding.

The cluster weight change relative to the combined effect of the bleeding and cooking was calculated as follows:

$$\Delta Cluster_{cooked}\ (\%) = ((W_{CC} - W_{CR}) / W_{CR}) \times 100 \quad (8)$$

where W_{CC} is the weight of a single cluster after cooking, cooling, and drainage.

2.3.2. Analyses of raw leg meat, cooked leg meat, and raw hepatopancreas

Samples of raw leg meat from all feeding groups, including the references from 2022 and 2023, were collected for differential scanning calorimetry (DSC) analysis and stored at -80 °C. Prior to the analysis, the tissue was thawed at 4 °C overnight. A subsample of 65 mg was extracted from each sample (n=3), placed into a Ø 7 mm medium pressure 120 µl crucible and hermetically sealed. A similar crucible with 50 mg deionized water, corresponding to the approximate weight of water in the samples, was used as a reference. The samples were analyzed in a DSC with an intercooler (DSC 1, Mettler Toledo, Switzerland) ranging from 10 °C to 120 °C at a heating rate of 10 °C/min. The resulting enthalpy curves were analyzed (software Star ver. 14, Mettler Toledo, Switzerland) for denaturation enthalpy (Δh) and peak maximum temperature (T_{max}) for each of the peaks observed using a baseline defined by a spline function and with start and endpoints determined as described by Skipnes et al. (2008). The peak with the highest T_{max} was observed around ~86 °C and is the one that will be focused on in this study.

Proximate chemical composition of the feed, cooked RKC leg meat and raw hepatopancreas were analyzed by the Nofima BioLab accredited laboratory. Crude protein was analyzed using the Kjeldahl method (($N \times 6.25$); ISO 5983–2, 2009), dry matter was determined gravimetrically after drying at 103 ± 1 °C (ISO 6496, 1999), total ash was determined by combustion of organic matter at 550 °C and gravimetric measurement of the residue (ISO 5984-2022), and crude lipid was measured according to Bligh and Dyer (1959). Before the analyses, the RKC sample tubes (50 mL) were stored at -40 °C. The tubes were thawed at 4 °C for 12 h and the sample material was mashed using an Ultra-Turrax® (IKA T25, Staufen, Germany).

The fatty and amino acids were analyzed as previously described (Kousoulaki et al., 2016). Briefly, the preparation of fatty acid methyl esters (FAMEs) for the determination of fatty acid composition was performed according to the AOCS Official Method Ce 1b-89 by trans-esterification of Bligh & Dyer extracted oils using a trace GC gas chromatograph (Thermo Fisher Scientific) with flame ionization detector (GC–FID), equipped with a 60 m × 0.25 mm BPX-70 cyan propyl column with 0.25 µm film thickness (SGE, Ringwood, Victoria, Australia). The sample solution (3.0 µl) was injected split-less, and the split was opened after 2 min. The FAMEs were identified by comparing the elution pattern and relative retention time with the reference FAME mixture (GLC-793, Nu-Chek Prep Inc., Elysian, MN, USA). Chromatographic peak areas were corrected by empirical response factors calculated from the areas of the GLC-793 mixture. Then, the fatty acid composition was estimated using 23:0 FAMEs as the internal standard and reported on a sample basis as g/100 g FAMEs. For the amino acid composition, the samples were hydrolyzed in 6 M HCl for 22 h at 110 °C and analyzed by HPLC using a fluorescence detection technique (Cohen and Michaud, 1993). Dietary gross energy was determined using a Parr adiabatic bomb calorimeter.

The proximate chemical composition, including amino acids, was expressed as a percentage of wet sample weight and fatty acid composition as a percentage of crude lipid weight. The measurements were averaged across samples obtained from up to six RKCs per feeding group, including the references from 2022 and 2023.

2.4. Statistics

The statistical analyses were performed by considering each RKC as a biological replicate. The values reported for each measured variable are the mean and standard deviation from the analyses conducted on each RKC.

The statistical significance of differences in the quality and processing parameters between feeding groups were analyzed by one-way analysis of variance (ANOVA) followed by *posthoc* pairwise multiple comparisons (Scheffé's test) using the software SYSTAT™ (vers. 13.2, Systat Software Inc., Palo Alto, CA, USA). Similarly, a one-way ANOVA followed by Dunnett's test was carried out to test if differences between the results for RKCs of the wild group from 2022 and 2023, respectively, were statistically significant.

We ran a principal component analysis (PCA) using Unscrambler (ver. 11, CAMO Software AS, Oslo, Norway), on the P20 and P100 groups, to simplify and visualize trends in the high dimensional multivariate measurements. These groups were selected to compare the effect of a low and high share of dry feed in the diet. Response variables for the PCAs included i) the morphology and processing attributes, ii) fatty acid composition for the cooked leg meat, and iii) fatty acid composition for the raw hepatopancreas.

The statistical analyses were performed at a 95% confidence level ($\alpha = 0.95$).

3. Results and discussion

3.1. Mortality and feeding

After the 12 months of feeding, the RKCs in the feeding groups P0, P20, P50, P80, and P100 showed a mortality rate 24.4%, 11.1%, 8.8%, 3.3% and 3.3%, respectively (10% on average across all feeding groups). Irrespective of the feeding group, mortality occurred in all months except Oct-Dec and peaked during molting (Jan-Feb). A high proportion of shrimp in the diet seemed to promote survival, since the first observations of mortality in the P0 group did not occur until after seven months when molting started. Although studies on mortality in feeding juvenile RKCs are scarce, general experience suggests that a mortality rate of 10% can be considered low. The *ad libitum* feeding (i.e., feeding in excess every Monday, Wednesday, and Friday) is a likely contributor to the low mortality rate, by promoting lower competition for food and decreased aggressiveness among the individuals. The most probable causes of elevated mortality during the molting period are unsuccessful molting and mortality due to cannibalism of newly molted individuals.

The juvenile RKCs were typically inactive when observed during the daytime. However, a sharp increase in activity, such as foraging and competing for feed, was observed during the feeding sessions. Similar activity observations were previously reported in a study with adult RKCs kept for 30 days (Borisov et al., 2007).

Feed remnants of shrimp and dry feed in varying amounts were observed the day after feeding. Shrimp leftovers were especially noticeable in the P0 and P20 groups, which could imply a reduced appetite for shrimp amongst the RKCs in those groups. After introducing sand into the tanks, the RKCs began digging and chewing on it. Comparable to a previous study, access to the sea sand showed positive effects on the juveniles' HSI, AI, MC, and shell thickness metrics (Lorentzen et al., 2023). Previous studies found evidence of sand or sediments in the stomachs of king crabs (Cunningham, 1969; Jewett and Feder, 1982; Jewett et al., 1990). It is suggested that the consumption of sand is a method to search for small crustaceans when larger prey is unavailable (Cunningham, 1969). It is hypothesized that the juveniles' instinct for searching for feed is stimulated when they have access to sea sand.

During the 12-month feeding period, the minimum and maximum seawater temperatures ranged from 3.5 °C in April to 10.8 °C in September. This temperature range is within their natural habitat (Christiansen et al., 2015); hence, it is not considered critical. The use of seawater at ambient temperature is also beneficial from an economic perspective, as it avoids the additional energy cost of cooling the water.

3.2. Growth performance and morphology

Growth performance was measured as the crab weight, CW, HSI, MC,

AI, shell thickness, and BI, given for the fed and the reference crabs (Table 1). Based on carapace length (CL) and CW from June 2022, a relationship of CL= 0.9038×CW was obtained ($R^2 = 0.9996$). The molt increment (MI), which is the absolute carapace size increase at molting for an individual (Hartnoll, 1982), was calculated using the CL equation. The MI ranged from 20.32 to 24.19 mm across the feeding groups. Corresponding numbers for the MI for RKCs captured near Kodiak Island ranged from 16.4 to 18.4 mm (Powell, 1967). Although not directly comparable, the large MI observed in this study indicates that controlled feeding of RKC juveniles did promote their growth.

The hepatopancreas index (HSI) and the meat content (MC) differed significantly ($p < 0.05$) among the feeding groups (Table 1). The HSI is an indicator of the biological and nutritional status of the RKC (Albalat et al., 2019). Increasing shares of dry feed in the diet led to decreasing HSI and MC values ($p < 0.05$), indicating suboptimal nutritional conditions for the crabs. This inference is further supported by observations made during the feeding periods, as the juveniles showed greater interest in the shrimps than in the dry feed in the P20, P50, and P80 groups. This could be due to the differences between these two feed items, especially regarding their size and texture, which affected the ability of the crabs to forage on them.

It was also observed that the RKC's had trouble gripping the dry feed, often requiring numerous attempts before they were able to grip the pellets. Once gripped, there was also a tendency for the pellets to crumble, limiting the ability of the juveniles to obtain a sufficient nutrition uptake. By contrast, the raw shrimps were more resilient and could be gripped several times without crumbling. A more effective and controlled uptake of the raw shrimp was assumed to occur due to the RKCs' ability to grip the shrimp with one chela, tear it into small pieces, and put it into the mouth using the other chela.

Previous studies have observed a decrease in the MC during live holding of adult RKCs without access to feed for up to three months (Lorentzen et al., 2019). In this study, the HSI decreased before the MC decreased, i.e., the RKCs used the energy reserves from the hepatopancreas before the muscle. This reflects the RKC strategies for utilizing the energetic reserves, lipids, and proteins.

Compared to the fed RKCs, the HSI for the wild RKCs for 2023 and the MC for 2022 and 2023 were significantly higher ($p < 0.05$). Apart from the challenges with the crumbling of the dry feed, this clearly shows the potential to further improve the diet to obtain HSI and MC values more comparable to the wild RKCs. Possible parameters to optimise include the ratio of dry feed vs. the raw shrimp, nutritional and textural profile of the dry feed, diet composition (exploring other marine by-products as feed components), feeding frequency, and location (single or multiple feeding locations within a single live holding tank). Reducing the feeding frequency is relevant as the RKCs in their natural habitats must cope with the scarcity or total absence of food for short or extended periods.

The abdomen index, AI, decreased significantly ($p < 0.05$) with an increasing share of dry feed in the diet. Like the HSI and MC, the AI reflects the overall well-being and condition of the animal. For the fed groups, the AI was significantly lower ($p < 0.05$) than for the reference RKCs from 2022 and 2023, although it is unclear if this is related to the diet composition, a lower feed intake due to the crumbling of the dry feed, or a combination of these two factors.

Although no significant differences in the shell thickness of the RKCs between the feeding groups, a thinner shell, on average, was observed, according to an increasing share of dry feed. Crustaceans generally need dietary sources of minerals primarily due to the molts (Saborowski, 2015). In a previous study, RKCs with access to sea sand obtained a thicker shell than those without sea sand (Lorentzen et al., 2023). As all groups had access to sea sand, the differences are assumed to reflect the nutritional conditions of the RKCs in the P80 and the P100 groups, as described earlier.

The browning index, BI, of the raw hepatopancreas increased with an increasing share of dry feed in the diet. The P80 group obtained a significantly ($p < 0.05$) higher BI than the P0 groups, and the P100 had higher BI ($p < 0.05$) than the P0, P20, and P50 groups. The variation could be explained by poorer nutritional conditions for the P80 and P100 crabs. The P80 and P100 crabs also showed higher standard deviations in BI than the other groups (Table 1). A possible explanation is that low access to nutrition could lead to the establishment of a hierarchy among the individuals in these groups, thereby leading to varying degrees of utilization of the lipid reserves. Conceivably, different utilization rates could lead to heterogeneity of the colors of the hepatopancreas of different crabs. However, the reference crabs from 2022 and 2023 had low and high BI values, respectively, while also having higher crude lipid content, on average, than the RKCs from the P100 group (Table 2). Thus, the type of feed offered appears to have a stronger effect on BI than different lipid utilization rates. To our knowledge, similar analyses and calculations of the BI of raw hepatopancreas from fed crustaceans have not been reported.

3.3. Processing attributes and proximate composition

Similarly to the decrease in HSI, MC, and AI, the cluster yield after cooking and the relative weight change after cooking changed according to an increased share of dry feed in the diet (Table 1). After the bleeding step, the cluster yield (CY_{raw}) did not differ significantly ($p > 0.05$). This is most likely due to the retention of the FBF within the structure of the muscle tissue (Mizuta et al., 2001). However, after the cooking, the cluster yield (CY_{cooked}) decreased due to a higher share of dry feed in the diet. A drop in the cooked cluster yield and MC was also observed due to the absence of feed for up to 3 months (Lorentzen et al., 2019). Regarding the MC drop, it was hypothesized that changes in the microstructure of the meat occurred, leading to an elevated liquid loss of loosely bound water, which became apparent after the cooking step.

Liquid loss during cooking is a major concern because it leads to a lower product weight and reduces the eating quality. In addition to water, minerals (e.g., sodium) and soluble proteins may also be lost in the process. Potential mechanisms for liquid loss include osmotic pressure, mass diffusion due to internal pressure during heating, and protein denaturation (Blikra et al., 2019; Skipnes, 2011). Protein denaturation causes liquid loss due to both shrinkage of the muscle, causing expulsion of extracellular moisture, and reduced water binding capacity of the proteins (Bell et al., 2001; Skipnes, 2011).

The denaturation peak for the RKC muscle, around 86 °C, was determined for all the groups applying DSC (Table 1). An endothermic peak around this temperature, associated with denaturation of actin, has been identified in several kinds of seafood previously, e.g., cod (Skipnes 2008) and Patagonian marine crabs (Dima et al. 2012). Although there were no significant differences between the feeding groups, the average denaturation peak temperature decreased due to an increasing share of dry feed in the diet. This is probably due to the reduction in the muscle volume as a response to lack of nutrition, observed as decreasing MC and yield (cooked). The decrease in denaturation temperature also implied elevated liquid loss ($\Delta Cluster_{cooked}$). A similar pattern of elevated liquid loss after cooking RKC clusters after 60 and 90 days with no feeding has been observed (Lorentzen et al., 2019).

A PCA was performed to visualize trends in the multivariate morphological and processing attributes (Fig. 1). The first (PC-1) and the second (PC-2) principal components accounted for 47% and 19% of the variance, respectively. The P20 and P100 feed groups plot as distinct and almost linearly separable groupings along PC-1 axis of the score plot (Fig. 1A). Except for the raw cluster yield (CY_{RAW}), weight, carapace width (CW), and shell thickness (SHELLTHKNS), the variance of the remaining parameters was well explained along PC-1 (Fig. 1B). Since the groups receiving different diets, P20 and P100, are almost separable along PC-1 there must be a strong correlation between diet and the morphological and processing attributes that are highly weighted in PC-1. This would be T4max, delta cooked (DELTACOOKE), cluster yield cooked (CYCOOKED), AI (ABDINDX), MC, and HSI (HSINDX). A

Table 2
Proximate chemical composition (%) in cooked leg meat and raw hepatopancreas of reference juveniles before starting the feeding (Wild 2022, *n*=20), reference juveniles for the 2023 sampling (Wild 2023, *n*=10), and after feeding for 12 months. The feeding groups include shrimps only (P0, n=5), 80% shrimps and 20% dry feed (P20, n=5), 50% shrimps and 50% dry feed (P50, n=5), 20% shrimps and 80% dry feed (P80, n=5), and 100% dry feed (P100, n=5).

	Wild RKCs 2022	***Wild RKCs 2023***	***Feeding groups***				
			P0	P20	P50	P80	P100
Cooked leg meat							
Moisture	81.23 ± 0.83	80.24 ± 0.56	81.22 ± 0.74	81.22 ± 0.74	81.94 ± 1.38^{X}	81.98 ± 0.74^{X}	80.46 ± 0.26
Total dry matter	18.77 ± 0.83	19.76 ± 0.56	18.78 ± 0.74	18.90 ± 0.80	18.06 ± 1.38^{X}	18.02 ± 0.74^{X}	19.54 ± 0.26
Total ash	1.48 ± 0.12	1.78 ± 0.04	2.02 ± 0.13$^{\Delta}$	1.90 ± 0.12$^{\Delta}$	2.08 ± 0.13$^{\Delta X}$	1.98 ± 0.04$^{\Delta X}$	2.06 ± 0.09$^{\Delta X}$
Crude protein	16.02 ± 0.61	16.00 ± 0.87	15.00 ± 0.86	14.90 ± 0.61	14.82 ± 0.92	15.26 ± 0.94	16.12 ± 0.76
Crude lipid	1.41 ± 0.10	1.18 ± 0.23	1.28 ± 0.13	1.26 ± 0.11	1.16 ± 0.09$^{\Delta}$	1.12 ± 0.15$^{\Delta}$	1.20 ± 0.07$^{\Delta}$
Raw hepatopancreas							
Moisture	56.34 ± 1.75	63.16 ± 4.08	62.94 ± 7.72	59.04 ± 0.93	67.1 ± 4.22$^{\Delta}$	64.62 ± 1.80$^{\Delta}$	69.0 ± 7.79$^{\Delta}$
Total dry matter	43.63 ± 1.75	36.84 ± 4.08	37.06 ± 7.72	40.96 ± 0.93	32.9 ± 4.22$^{\Delta}$	35.38 ± 1.80$^{\Delta}$	31.00 ± 7.79$^{\Delta}$
Total ash	1.58 ± 0.08	1.78 ± 0.13	1.74 ± 0.23	1.72 ± 0.08	1.98 ± 0.15$^{\Delta}$	1.9 ± 0.12$^{\Delta}$	1.96 ± 0.25$^{\Delta}$
Crude protein	11.85 ± 0.65	14.0 ± 0.57	12.48 ± 1.16	12.78 ± 0.58	13.64 ± 0.87	14.0 ± 0.81$^{\Delta}$	13.4 ± 2.09
Crude lipid	29.23 ± 2.90	19.16 ± 5.15	22.14 ±7.19^{ab}	25.66 ± 0.93^{a}	16.78 ± 4.49$^{ab\Delta}$	18.38 ± 2.98$^{ab\Delta}$	14.34 ± 5.50$^{b\Delta}$

Note. Results are expressed as mean values (± standard deviation). Different superscript letters within the same row of the fed RKCs indicate significantly different mean values ($p < 0.05$, full factorial ANOVA followed by Scheffe's test). The symbol Δ and X indicates the mean values significantly different ($p < 0.05$. One-way ANOVA followed by Dunnett's test) from the mean value observed for wild crabs in 2022 and 2023, respectively.

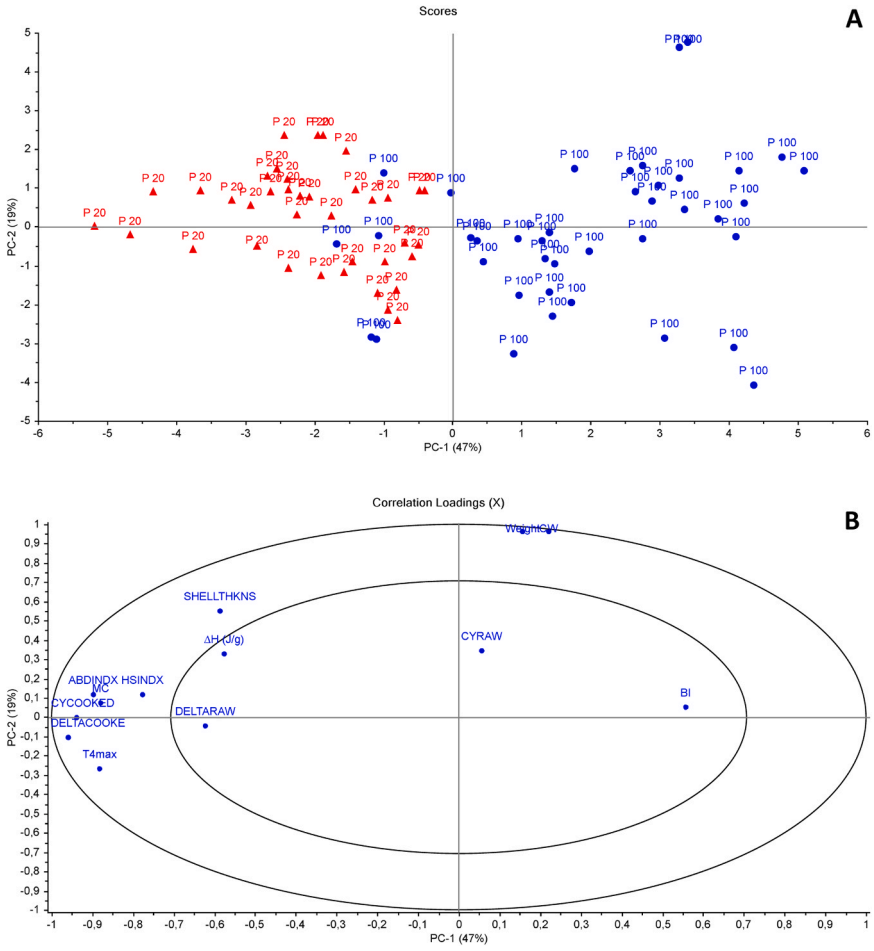

Fig. 1. Score plot (A) with observations grouped by the feeding groups P20 and P100. The correlation loading plot (B) shows the correlation between the response variables Weight (g), CW (cm), ABDINDEX, abdomen index, HSINDX, hepatopancreas index, BI, browning index of the hepatopancreas, SHELLTHKNS, shell thickness, CYRAW, cluster yield raw; CYCOOKED, cluster yield cooked; DELTA RAW, DELTA COOKED, ΔH (J/g), and $T4_{max}$. The outer and inner ellipse indicate 100% and 50% explained variance, respectively.

correlation between the AI and the MC along PC-1 was observed (Fig. 1B). A similar relationship was described by the Siikavuopio et al. (2011), and it was suggested that AI metrics could be used to indicate the leg meat content.

On the other hand, the variability in crab weight and CW are mostly explained by PC-2, which shows no correlation with the type of feed. Although not measured, these parameters might be coherent to a variety of feed consumed but might also be due to genetic differences as found in Chinese mitten crab (Liu et al., 2018). Growth measured in terms of increasing crab weight and CW are the two most important metrics for

assessing the success of feeding juveniles in captivity.

The proximate composition of the cooked leg meat and raw hepatopancreas from the feeding groups (P0 – P100) and the references are presented in Table 2. No significant differences ($p > 0.05$) in any of the analyzed parameters were detected in the leg meat among the feeding groups. For some feeding groups, the moisture, total dry matter, total ash, and crude proteins differed significantly ($p < 0.05$) from the corresponding values for the reference crabs but with no clear pattern. The crude lipid content in the hepatopancreas of the P100 group was significantly ($p < 0.05$) lower than in the P20 group. A low lipid content in the P100 group supports the inference of suboptimal nutritive conditions. When energy intake through foraging is insufficient, crustaceans must rely on their energetic reserves, i.e., protein, glycogen, and lipid, to ensure metabolic functionality (McLeod et al., 2004; Sacristán et al., 2017). The low lipid content of the hepatopancreas in the P100 group shows that the juveniles needed to utilize their body reserves to compensate. Similar observations of reduced lipid content in the hepatopancreas of adult RKCs were observed by Lian et al. (2022) for RKCs that were kept in a live holding regime without feeding for 3 months. In addition to the reduced lipid content of the hepatopancreas, the protein content in the cooked leg meat was also reduced (Lian et al. 2022), while in the present study, the protein content of the leg meat did not differ significantly ($p < 0.05$) among the feeding groups. This reflects the sequence of the utilization of reserves, i.e., the crabs kept without feeding for three months began to utilize the energy stored as protein, while the crabs in the present study did not have to utilize this reserve.

3.4. Fatty acids

After feeding the crabs for 12 months, we observed significant variation in fatty acid composition in the cooked leg meat and raw hepatopancreas between feeding groups (Table 3). The identified fatty acids ranged from 51% to 58% and 69–85% for the leg meat and raw hepatopancreas, respectively. The fatty acid composition of the leg meat and the raw hepatopancreas also differed irrespective of the feeding groups and reference groups. Lower levels of MUFA (monounsaturated fatty acids) were consistently measured in leg meat compared to the hepatopancreas. By contrast, the levels of PUFAs (polyunsaturated fatty acids) were consistently higher in the leg meat than in the hepatopancreas. This is in accordance with the observations published by Lian et al. (2022). The MUFAs are assumed to function as long-term storage lipids, while the PUFAs function as structural lipids (Sacristán et al., 2017).

In the cooked leg meat, the most abundant fatty acids were palmitic (C16:0), C18:1 ($n9$) + ($n7$) + ($n5$), arachidonic (ARA), eicosapentaenoic (EPA), and docosahexaenoic (DHA) acid. The most abundant fatty acids in the raw hepatopancreas were palmitic, palmitoleic (C16:1$n7$), C18:1 ($n9$) + ($n7$) + ($n5$), C20:1 ($n9$) + ($n7$), EPA, C22:1 ($n11$) + ($n9$) + ($n7$), and DHA. Across all the feeding groups, the fatty acids in the leg meat can be grouped as PUFA, MUFA, and SFA in descending order of abundance. A PCA was performed to provide a visual overview of the fatty acids in cooked leg meat (Fig. 2) and raw hepatopancreas (Fig. 3) from the feeding groups P20 and P100. For the cooked leg meat, the first (PC-1) and the second (PC-2) principal components accounted for 47 and 17% of the variance, respectively (Fig. 2). The P20 and P100 plot as distinct clusters and are separable along the PC-1 axis (Fig. 2A). Of the most abundant fatty acids for the leg meat, C18:1 ($n9$) + ($n7$) + ($n5$), ARA, and EPA were more abundant for the P20 than for the P100 group (Table 3 and Fig. 2B).

For the raw hepatopancreas, the first (PC-1) and second (PC-2) principal components accounted for 64 and 15% of the variance, respectively (Fig. 3). Similarly to the cooked leg meat, a clustering of the P20 and P100 groups and separability along the PC-1 axis was observed (Fig. 3A). The most abundant fatty acids were C16:1$n7$, C18:1 ($n9$) + ($n7$) + ($n5$), EPA, and DHA and these were more abundant for the P20 group than for the P100 group. On the other hand, palmitic acid and C22:1 ($n11$) + ($n9$) + ($n7$) had higher abundance for the P100 group than for the P20 group. The dominant type of fatty acids in the raw hepatopancreas for the fed groups, including the reference from 2022, were MUFA, the second most common fatty acid type were PUFA, and the third most common were SFA. By contrast, MUFA and PUFA both had similar abundances in the reference RKCs from 2023, suggesting that the type of food items consumed affects fatty acid composition. A previous study by Dvoretsky et al. (2020) on fatty acids in the hepatopancreas from RKCs from the Barents Sea found that the dominant type was PUFA, followed by SFA and MUFA, supporting the interpretation of diet controlled variation.

It is important to note that the differences in fatty acid composition between the P20 and P100 groups could be explained by diet composition, reduced nutritional status due to the crumbling of the dry feed, or a combination of these two factors. It is challenging to disentangle these factors and unambiguously conclude how diet affects fatty acid composition without knowing the exact amount and type of feed consumed. For farmed Atlantic Salmon, the fatty acid composition is affected by the fatty acid composition of the oils used in the dry feed (Torstensen et al., 2000). To explore possible similar effects in RCKs, the crabs must be fed with dry feeds with different fatty acid compositions in conditions where feed intake is controlled and measured.

3.5. Amino acids

The amino acid composition of the cooked leg meat and raw hepatopancreas from the feeding groups (P0 – P100) and the references are presented in Table 4. Arginine, aspartic acid, glutamic acid, leucine, and lysine were the major components in the cooked leg meat. Except for glycine, the amino acid composition of the cooked leg meat within the feeding groups did not differ significantly ($p > 0.05$). However, some deviation in AAs was observed when comparing the feeding groups with the reference crabs from 2023. Interestingly, the AA composition from the feeding groups with a high share of dry feed, i.e., P80 and P100, was most similar to the reference crabs from 2023. Except for the aspartic acid, the AA composition of the raw hepatopancreas did not differ significantly ($p > 0.05$) within the feeding groups. Irrespective of feeding groups, the proline concentration was significantly ($p < 0.05$) higher than for the reference crabs from 2022 and 2023.

The diets of crustacean species must contain ten essential amino acids (EAAs) for survival and growth: Arginine, methionine, valine, threonine, isoleucine, leucine, lysine, histidine, phenylalanine, and tryptophan, all of which are not synthesized *de novo* by eukaryotic cells (NRC, 2011). The raw shrimps and the dry feed contained these EAAs (Supplementary Table 2).

The molts of crustaceans are strongly influenced by feed intakes, indicating that AAs are required for tissue growth, especially in the postmolt (Nguyen et al., 2014). It has been hypothesized that the AAs are essential for the molting process through energy provision, osmoregulation, collagen synthesis, and the removal of the exoskeleton (Dooley et al., 2002; Li et al., 2021).

Like the fatty acid composition, not knowing the exact amount of dry feed consumed makes it challenging to unambiguously conclude the effect of diet (diet composition vs amount) on the AA composition of the cooked leg meat and the raw hepatopancreas. For farmed Atlantic Salmon, as for the fatty acids, the AA composition has been shown to be affected by the diet composition (Mente et al., 2003). An additional controlled growth trial is required to isolate the effect of diet composition on AA in RCKs.

3.6. General considerations

Irrespective of the diet's dry feed and raw shrimp ratio, our study has documented low mortality and the potential to double the weight of juvenile RKCs after 12 months of live holding. Despite clear indications of insufficient feeding of the juveniles, especially in the P100 group, our

Table 3
Fatty acid composition (g/100 g crude lipid) of cooked leg meat and raw hepatopancreas of reference juveniles before starting the feeding (Wild 2022, *n*=6), reference juveniles in 2023 (Wild 2023, *n*=5), and after feeding the juveniles for 12 months. The feeding groups includes 100% shrimps (P0, n=5), 80% shrimps and 20% dry feed (P20, n=5), 50% shrimps and 50% dry feed (P50, n=5), 20% shrimps and 80% dry feed (P80, n=5), and 100% dry feed (P100, n=5).

	Wild 2022	***Wild 2023***	***Feeding groups***				
			P0	P20	P50	P80	P100
Cooked leg meat							
(n-6)/(n-3)	0.20 ± 0.00	0.20 ± 0.00	0.14 ± 0.05$^{ab\Delta x}$	0.10 ± 0.00$^{a\Delta x}$	0.18 ± 0.04^{b}	0.20 ± 0.00^{b}	0.20 ± 0.00^{b}
C14:0	0.55 ± 0.05	0.40 ± 0.00	0.42 ± 0.08$^{a\Delta}$	0.38 ± 0.04$^{a\Delta}$	0.40 ± 0.07$^{a\Delta}$	0.48 ± 0.04^{a}	0.66 ± 0.13^{bx}
C16:0	8.85 ± 0.48	8.00 ± 0.50	9.74 ± 0.40$^{a\Delta x}$	8.98 ± 0.29^{ax}	8.68 ± 0.22^{ab}	8.86 ± 0.42^{abx}	9.50 ± 0.49^{ax}
C16:1n7	1.61 ± 0.13	1.80 ± 0.37	1.24 ± 0.25$^{a\Delta x}$	1.18 ± 0.13$^{a\Delta x}$	1.12 ± 0.13$^{ab\Delta x}$	0.94 ± 0.15$^{ab\Delta x}$	0.84 ± 0.05$^{b\Delta x}$
C16:2n4	<0.10	<0.10	<0.10	<0.10	<0.10	<0.10	<0.10
C16:3n4	<0.10	<0.10	<0.10	<0.10	0.28 ± 0.13	0.28 ± 0.04	0.10 ± 0.00
C18:0	1.78 ± 0.14	1.56 ± 0.05	1.60 ± 0.10$^{a\Delta}$	1.38 ± 0.04$^{b\Delta x}$	1.38 ± 0.08$^{b\Delta x}$	1.34 ± 0.09$^{b\Delta x}$	1.24 ± 0.09$^{b\Delta x}$
C18:1 (n9) + (n7) + (n5)	11.13 ± 0.98	9.08 ± 0.23	14.80 ± 0.72$^{a\Delta x}$	13.06 ± 0.21$^{b\Delta x}$	13.22 ± 0.23$^{b\Delta x}$	12.72 ± 0.77$^{b\Delta x}$	11.24 ± 0.32^{bcx}
C18:2n6	0.93 ± 0.28	0.64 ± 0.05	0.96 ± 0.13^{ax}	1.08 ± 0.15^{abx}	1.40 ± 0.16$^{b\Delta x}$	1.86 ± 0.15$^{c\Delta x}$	2.20 ± 0.2$^{c\Delta x}$
C18:3n3	0.25 ± 0.12	0.20 ± 0.00	0.38 ± 0.08^{x}	0.38 ± 0.08^{x}	0.38 ± 0.08^{x}	0.44 ± 0.09$^{\Delta x}$	0.48 ± 0.08^{x}
C18:3n6	0.10 ± 0.00	0.12 ± 0.04	<0.10	<0.10	<0.10	<0.10	<0.10
C18:4n3	0.27 ± 0.08	0.38 ± 0.04	<0.10	0.10 ± 0.00	0.10 ± 0.00	0.16 ± 0.05	0.18 ± 0.04
C20:0	<0.10	<0.10	<0.10	<0.10	<0.10	<0.10	<0.10
C20:1 (n9) + (n7)	1.63 ± 0.10	1.36 ± 0.23	1.66 ± 0.31	1.54 ± 0.26	1.52 ± 0.33	1.82 ± 0.23	1.52 ± 0.23$^{\Delta}$
C20:2n6	0.48 ± 0.04	0.48 ± 0.08	0.30 ± 0.00$^{a\Delta x}$	0.22 ± 0.04$^{b\Delta x}$	0.28 ± 0.04$^{ab\Delta x}$	0.30 ± 0.00$^{a\Delta x}$	0.30 ± 0.00$^{a\Delta x}$
C20:3n3	<0.10	<0.10	<0.10	<0.10	<0.10	<0.10	<0.10
C20:3n6	<0.10	<0.10	<0.10	<0.10	<0.10	<0.10	<0.10
C20:4n3	0.20 ± 0.00	0.24 ± 0.05	0.16 ± 0.05	0.18 ± 0.05	0.15 ± 0.06	0.16 ± 0.05	0.16 ± 0.05
C20:4n6 (ARA)	4.10 ± 0.21	3.16 ± 0.23	2.50 ± 0.19$^{a\Delta x}$	2.12 ± 0.19$^{b\Delta x}$	2.22 ± 0.26$^{ab\Delta x}$	1.88 ± 0.08$^{b\Delta x}$	1.76 ± 0.09$^{b\Delta x}$
C20:5n3 (EPA)	14.7 ± 0.40	12.18 ± 0.57	14.68 ± 0.49$^{a\Delta x}$	13.26 ± 0.42$^{b\Delta x}$	13.44 ± 0.43$^{bc\Delta x}$	13.04 ± 0.41$^{bde\Delta x}$	12.28 ± 0.28^{e}
C21:5n3	0.35 ± 0.05	0.34 ± 0.05	0.18 ± 0.04$^{\Delta x}$	0.17 ± 0.06$^{\Delta x}$	0.23 ± 0.13$^{\Delta}$	0.16 ± 0.05$^{\Delta x}$	0.17 ± 0.06$^{\Delta x}$
C22:0	<0.10	<0.10	<0.10	<0.10	<0.10	<0.10	<0.10
C22:1 (n11) + (n9) + (n7)	0.30 ± 0.09	0.15 ± 0.10	0.38 ± 0.13^{x}	0.42 ± 0.08^{x}	0.50 ± 0.14^{x}	0.50 ± 0.12^{x}	0.42 ± 0.13^{x}
C22:4n6	0.20 ± 0.00	0.12 ± 0.04	<0.10	<0.10	<0.10	<0.10	<0.10
C22:5n3	0.67 ± 0.12	0.60 ± 0.07	0.32 ± 0.04$^{\Delta x}$	0.30 ± 0.00$^{\Delta x}$	0.28 ± 0.04$^{\Delta x}$	0.30 ± 0.00$^{\Delta x}$	0.28 ± 0.04$^{\Delta x}$
C22:6n3 (DHA)	10.28 ± 0.59	10.28 ± 0.58	10.58 ± 0.64$^{\Delta}$	10.00 ± 0.41$^{\Delta}$	10.20 ± 0.50$^{\Delta}$	10.30 ± 0.52$^{\Delta}$	9.48 ± 0.80$^{\Delta}$
C24:1n9	<0.10	<0.10	<0.10	<0.10	<0.10	<0.10	<0.10
Sum (EPA + DHA)	24.98 ± 0.96	22.46 ± 0.92	25.24 ± 0.96^{ax}	23.28 ± 0.19$^{b\Delta}$	23.64 ± 0.33^{b}	23.34 ± 0.79$^{b\Delta}$	21.74 ± 0.89$^{c\Delta}$
Sum (n3) fatty acids	26.73 ± 0.91	24.34 ± 1.01	26.38 ± 0.97^{ax}	24.36 ± 0.19^{bc}	24.78 ± 0.39^{b}	24.60 ± 0.78^{b}	23.04 ± 0.94^{c}
Sum (n6) fatty acids	5.87 ± 0.33	4.60 ± 0.25	3.82 ± 0.15$^{ab\Delta x}$	3.52 ± 0.13$^{a\Delta x}$	3.94 ± 0.24$^{b\Delta x}$	4.12 ± 0.11$^{bc\Delta x}$	4.34 ± 0.15^{cx}
Sum PUFA	32.65 ± 1.14	29.00 ± 1.12	30.28 ± 0.86$^{a\Delta}$	27.92 ± 0.23$^{b\ \Delta}$	28.94 ± 0.57$^{ab\Delta}$	28.98 ± 0.77$^{ab\ \Delta}$	27.46 ± 1.07$^{b\Delta x}$
Sum identified fatty acid	58.73 ± 2.47	51.50 ± 0.76	60.18 ± 2.43^{ax}	54.98 ± 0.56^{bx}	55.88 ± 0.80^{bx}	55.78 ± 1.70^{bx}	53.08 ± 1.68^{b}
Sum saturated fatty acids	11.33 ± 0.55	10.12 ± 0.50	11.88 ± 0.49^{ax}	10.84 ± 0.24^{bx}	10.62 ± 0.26$^{b\Delta}$	10.76 ± 0.36b	11.52 ± 0.47^{ax}
Sum MUFA	14.72 ± 1.20	12.38 ± 0.40	18.02 ± 1.30$^{a\Delta x}$	16.18 ± 0.52^{bx}	16.36 ± 0.60$^{b\Delta x}$	16.00 ± 1.00^{bx}	14.08 ± 0.43^{bcx}
Sum unidentified fatty acid	6.03 ± 0.48	4.44 ± 0.23	3.42 ± 0.41	2.98 ± 0.45$^{\Delta}$	2.70 ± 0.79$^{\Delta}$	1.98 ± 0.20$^{\Delta}$	2.72 ± 0.29$^{\Delta}$
Raw hepatopancreas							
(n-6)/(n-3)	0.20 ± 0.00	0.20 ± 0.00	0.16 ± 0.05$^{\Delta x}$	0.20 ± 0.00	0.20 ± 0.00	0.20 ± 0.00	0.20 ± 0.00
C14:0	3.70 ± 0.37	1.34 ± 0.11	1.00 ± 0.31$^{a\Delta}$	1.16 ± 0.18$^{a\Delta}$	1.44 ± 0.51$^{a\Delta}$	2.34 ± 0.30$^{b\Delta x}$	2.92 ± 0.49$^{b\Delta x}$
C16:0	9.57 ± 0.20	8.54 ± 0.85	7.10 ± 1.25$^{a\Delta x}$	7.52 ± 0.63$^{ab\Delta}$	7.88 ± 0.85$^{ab\Delta}$	9.08 ± 0.37^{b}	9.06 ± 0.56^{b}
C16:1n7	4.75 ± 0.19	4.38 ± 1.08	3.28 ± 1.09$^{\Delta}$	3.64 ± 0.42$^{\Delta}$	3.62 ± 0.58$^{\Delta}$	3.34 ± 0.34$^{\Delta}$	2.84 ± 0.44$^{\Delta}$
C16:2n4	0.18 ± 0.04	<0.10	0.10 ± 0.00	0.10 ± 0.00	0.10 ± 0.00	0.10 ± 0.00	0.13 ± 0.05
C16:3n4	0.20 ± 0.00	0.12 ± 0.04	0.14 ± 0.05	0.10 ± 0.00$^{\Delta}$	0.16 ± 0.05	0.16 ± 0.05	0.18 ± 0.04
C18:0	1.40 ± 0.17	2.46 ± 0.15	1.56 ± 0.27^{x}	1.48 ± 0.13^{x}	1.48 ± 0.19^{x}	1.38 ± 0.08^{x}	1.34 ± 0.05^{x}
C18:1 (n9) + (n7) + (n5)	15.67 ± 0.58	13.72 ± 0.83	29.34 ± 1.47$^{a\Delta x}$	28.46 ± 1.05$^{ab\Delta x}$	26.30 ± 1.66$^{b\Delta x}$	23.06 ± 0.55$^{c\Delta x}$	18.94 ± 0.77$^{d\Delta x}$
C18:2n6	1.03 ± 0.05	0.88 ± 0.08	1.04 ± 0.13^{a}	1.26 ± 0.11^{abx}	1.58 ± 0.36$^{b\Delta x}$	2.54 ± 0.11$^{c\Delta x}$	2.90 ± 0.17$^{c\Delta x}$
C18:3n3	0.58 ± 0.04	0.52 ±0.04	0.56 ± 0.15	0.62 ± 0.04	0.64 ± 0.17	0.78 ± 0.04$^{\Delta x}$	0.78 ± 0.11$^{\Delta x}$
C18:3n6	0.12 ± 0.04	0.26 ± 0.05	0.20 ± 0.00	0.20 ± 0.00	0.14 ± 0.05	0.10 ± 0.00	<0.10
C18:4n3	1.42 ± 0.19	1.90 ± 0.14	0.42 ± 0.13$^{a\Delta x}$	0.52 ± 0.04$^{ab\Delta x}$	0.54 ± 0.17$^{ab\Delta x}$	0.70 ± 0.07$^{b\Delta x}$	0.76 ± 0.15$^{b\Delta x}$
C20:0	0.10 ± 0.00	0.18 ± 0.04	0.10 ±0.00	0.10 ± 0.00	0.10 ± 0.00	<0.10	<0.10
C20:1 (n9) + (n7)	11.78 ± 0.77	8.12 ± 0.46	12.72 ± 2.46^{x}	11.80 ± 1.34^{x}	10.80 ± 1.18^{x}	11.70 ± 0.27^{x}	12.22 ± 1.19^{x}
C20:2n6	0.65 ± 0.05	1.52 ±0.25	0.60 ± 0.12^{ax}	0.54 ± 0.05^{abx}	0.54 ± 0.05^{abx}	0.44 ± 0.05$^{b\Delta x}$	0.38 ± 0.04$^{b\Delta x}$
C20:3n3	0.10 ± 0.00	0.20 ± 0.00	0.28 ± 0.04$^{ab\Delta x}$	0.32 ± 0.04$^{a\Delta x}$	0.26 ± 0.05$^{ab\Delta x}$	0.20 ± 0.00$^{b\Delta}$	0.10 ± 0.00^{cx}
C20:3n6	<0.10	0.10 ± 0.00	<0.10	<0.10	<0.10	<0.10	<0.10
C20:4n3	0.50 ± 0.00	0.68 ± 0.15	0.36 ± 0.09$^{\Delta x}$	0.40 ± 0.00$^{\Delta x}$	0.34 ± 0.05$^{\Delta x}$	0.38 ± 0.04$^{\Delta x}$	0.36 ± 0.05$^{\Delta x}$
C20:4n6 (ARA)	1.28 ± 0.18	2.48 ± 0.18	1.10 ± 0.10$^{a\Delta x}$	0.98 ± 0.11^{ax}	1.18 ± 0.24^{ax}	0.60 ± 0.07$^{b\Delta x}$	0.46 ± 0.13$^{b\Delta x}$
C20:5n3 (EPA)	6.67 ± 0.29	7.46 ± 0.62	5.72 ± 1.77^{abx}	6.38 ± 0.84^{ab}	6.54 ± 1.01^{a}	4.94 ± 0.19$^{ab\Delta x}$	4.32 ± 0.50$^{b\Delta x}$
C21:5n3	0.33 ± 0.05	0.50 ± 0.07	0.18 ± 0.05$^{\Delta x}$	0.20 ± 0.00$^{\Delta x}$	0.20 ± 0.00$^{\Delta x}$	0.20 ± 0.00$^{\Delta x}$	0.20 ± 0.00$^{\Delta x}$
C22:0	<0.10	<0.10	<0.10	<0.10	<0.10	<0.10	<0.10
C22:1 (n11) + (n9) + (n7)	11.30 ± 1.04	1.10 ± 0.26	8.68 ± 1.14$^{a\Delta x}$	8.82 ± 1.09$^{a\Delta x}$	8.90 ± 1.07$^{a\Delta x}$	10.88 ± 0.72^{abx}	12.78 ±1.47^{bx}
C22:4n6	0.23 ± 0.05	0.46 ± 0.05	0.10 ± 0.00	0.10 ± 0.00	<0.10	<0.10	<0.10
C22:5n3	0.82 ± 0.08	1.00 ± 0.14	0.62 ± 0.04$^{\Delta x}$	0.58 ± 0.04$^{\Delta x}$	0.60 ± 0.00$^{\Delta x}$	0.60 ± 0.00$^{\Delta x}$	0.60 ± 0.00$^{\Delta x}$
C22:6n3 (DHA)	10.17 ± 0.61	11.64 ± 0.91	10.2 ± 0.98^{x}	10.24 ± 0.42^{x}	10.34 ± 1.02^{x}	9.92 ± 0.47^{x}	9.24 ± 0.30^{x}
C24:1n9	0.40 ± 0.00	0.10 ± 0.00	0.30 ± 0.07$^{a\Delta\ x}$	0.38 ± 0.04^{abx}	0.36 ± 0.05^{abx}	0.44 ±0.05^{bx}	0.46 ± 0.09^{bx}
Sum (EPA + DHA)	16.83 ± 0.57	19.08 ± 1.25	15.94 ± 2.63^{x}	16.6 ± 1.24	16.88 ± 1.95	14.88 ±0.50^{x}	13.54 ± 0.23$^{\Delta x}$
Sum (n3) fatty acids	20.60 ± 0.49	23.88 ± 1.48	18.34 ± 3.01^{x}	19.22 ± 1.28^{x}	19.46 ± 2.11^{x}	17.70 ±0.38$^{\Delta x}$	16.38 ± 0.13$^{\Delta x}$
Sum (n6) fatty acids	3.45 ± 0.26	5.70 ± 0.50	3.08 ± 0.11$^{a\Delta x}$	3.10 ± 0.17$^{a\Delta x}$	3.56 ± 0.11^{bx}	3.76 ± 0.05$^{bc\Delta x}$	3.86 ± 0.05$^{c\Delta x}$
Sum PUFA	24.40 ± 0.57	29.78 ± 1.88	21.64 ± 2.98$^{\Delta x}$	22.58 ± 1.42^{x}	23.30 ± 2.20^{x}	21.74 ± 0.36$^{\Delta x}$	20.54 ± 0.15$^{\Delta x}$
Sum identified fatty acid	83.13 ± 1.41	69.80 ± 1.42	85.74 ± 2.10^{x}	85.94 ± 0.62^{ax}	84.16 ± 2.11^{x}	84.08 ± 1.03^{x}	81.30 ± 5.12^{x}
Sum saturated fatty acids	14.85 ± 0.36	12.64 ± 1.03	9.78 ± 1.83$^{a\Delta x}$	10.26 ± 0.92$^{a\Delta x}$	10.92 ± 1.37$^{ab\ \Delta}$	12.92 ± 0.61$^{b\ \Delta}$	13.48 ± 1.09^{b}
Sum MUFA	43.87 ± 1.43	27.44 ± 2.09	54.34 ± 3.51$^{a\Delta x}$	53.06 ± 2.64$^{ab\Delta x}$	49.94 ± 2.69$^{ab\Delta x}$	49.40 ± 0.74$^{ab\Delta x}$	47.26 ± 4.00^{bx}
Sum unidentified fatty acid	8.50 ± 0.93	13.00 ± 1.17	4.20 ± 0.41$^{\Delta x}$	4.26 ± 0.24$^{\Delta x}$	4.32 ± 0.41$^{\Delta x}$	4.16 ± 0.11$^{\Delta x}$	4.18 ± 0.24$^{\Delta x}$

Note. Results are expressed as mean values (± standard deviation). Different superscript letters within the same row for leg meat and hepatopancreas indicate significantly different mean values ($p < 0.05$. full factorial ANOVA followed by Scheffe's test). Furthermore, Δ and X indicate significant differences between the fed RKCs and the wild 2022 and wild 2023, respectively. ($p < 0.05$).
Abbreviations: ARA. EPA. PUFA. Polyunsaturated fatty acids; MUFA. Monoenoic fatty acids.

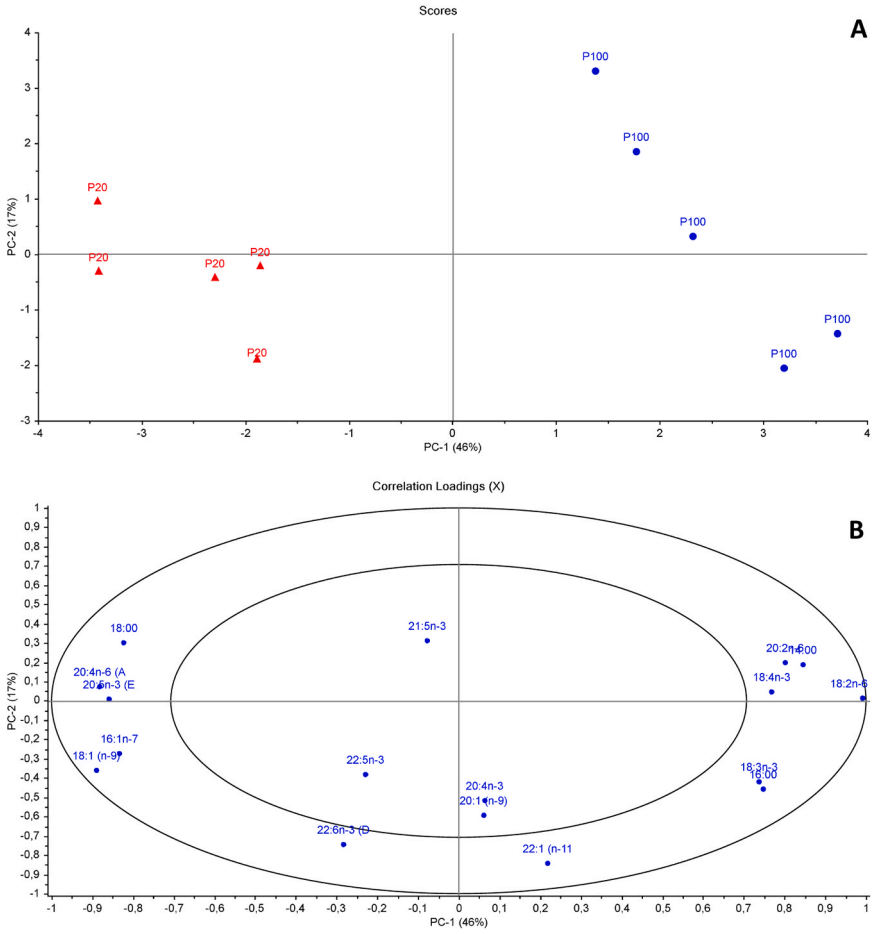

Fig. 2. Score plot (A) with fatty acids in the cooked leg meat grouped by the feeding groups P20 and P100. The correlation loading plot (B) shows the correlation between the response variables of the fatty acids. The outer and inner ellipse indicate 100% and 50% explained variance, respectively.

data show encouraging overall growth performance.

The dry feed showed high water stability but was not optimized to prevent crumbling during eating. A proper binder in dry feed production might mitigate the problem of crumbling. Furthermore, the shape of the dry feed could be optimized to improve the ability of the RCKs to grip the pellets. In previous studies, larger pellets of dry feed have been tested, and the ability to grip it improved (Siikavuopio et al., 2006). These pellets were not used in this experiment due to their high cost.

In groups with a low share of dry feed, remnants were often observed after the feeding period. Despite this, the RKCs from these groups obtained the best results for morphology and processing attributes. Fewer remnants but poorer morphology and processing attributes were observed for the RKCs in the groups with a high share of dry feed. Interestingly, while groups with a high share of shrimps in the diet gave the best morphology and processing attributes, they also had the highest mortality rates. The high share of raw shrimps in the diet was unfavorable in the long run since the increased mortality rate outweighed the favorable effects on morphology and processing attributes.

The results for the fed crabs are obtained from 110 to 170 days after the molting, i.e., late postmolt. The morphology and processing attributes may have been improved if the RKCs had been sampled, processed, and analyzed in October or November, i.e., during the intermolt stage. However, sampling during the intermolt stage could also suppress variations among the feeding groups since the typical condition of intermolt RKCs is good (Lian et al., 2021).

This study did not explore the specific feed intake for each individual. Hence, whether the results obtained reflect the diet composition, a lower feed intake due to pellet crumbling, or a combination of these factors is unknown. Apart from these uncertainties, the results of this study are promising and provide a basis for the continued development of dry feed to improve the quality of processed crab meat. Other feeding parameters to be optimized are i) the combination of dry feed and raw shrimp, ii) the feeding frequency, and iii) the feeding regimen, i.e., feeding at one or more locations in the live holding tank. Moreover, the nutritional composition of the feed could be varied and optimized according to the life stage of the crabs, including different stages in the molting cycle. Notably, altering the nutritional composition and binder strategy for improved crumbling properties can impact gastrointestinal filling, passage rate, and how effectively nutrients are hydrolyzed and adsorbed (Bogevik et al., 2021). Collection of uneaten feed and feces is necessary to calculate feed intake, conversion ratio, growth rate, and nutrient digestibility. This additional level of control is necessary to unravel the effects of intake quantity and diet composition on the overall growth performance of fed RKC juveniles.

While this study focused on dry feed and raw shrimps, alternative marine by-products such as herring, blue mussels, sea urchins, and

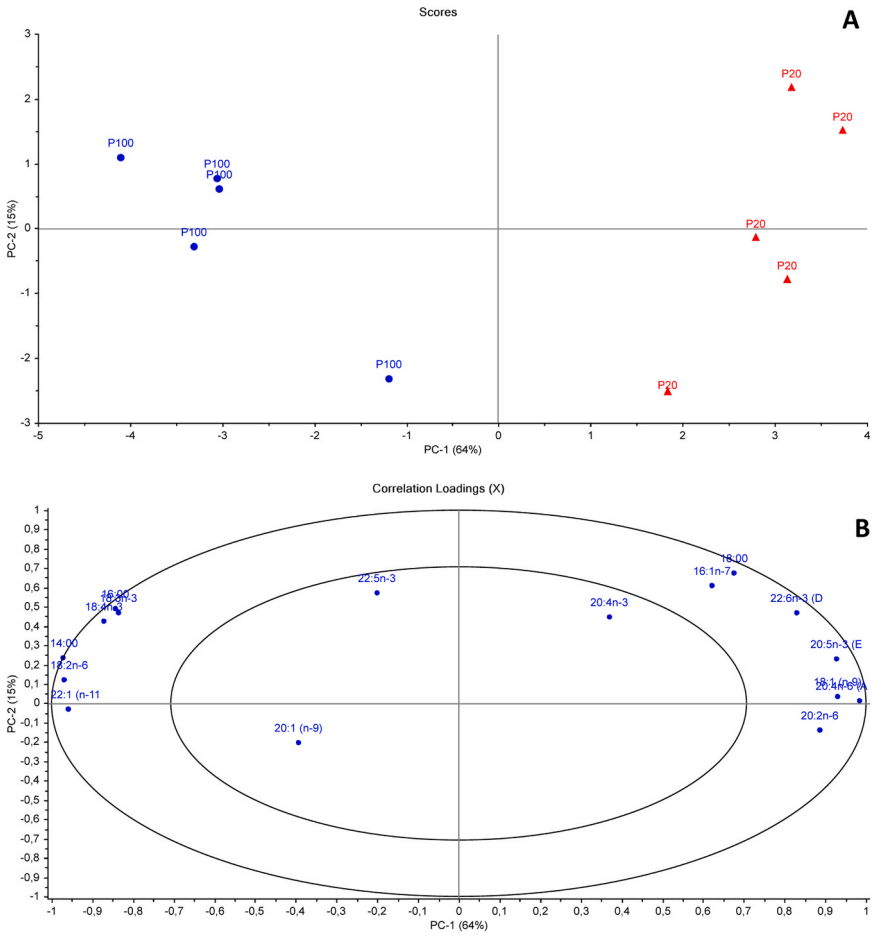

Fig. 3. Score plot (A) with fatty acids in the raw hepatopancreas grouped by the feeding groups P20 and P100. The correlation loading plot (B) shows the correlation between the response variables of the fatty acids. The outer and inner ellipse indicate 100% and 50% explained variance, respectively.

capelins (Lorentzen et al., 2023) and backbones of saith (pers. communication F. Lian, Nofima) have been used as feed for RKCs. The use of marine by-products promotes sustainable resource utilization and could also be combined with dry feed. If the live holding of juvenile RKCs is to become a successful industry, feeding with marine by-products could help to fulfill sustainability goals. In aquaculture programs, irrespective of species, the feed cost is a significant share of the total costs. Hence, relatively abundant and available marine by-products as feed components could be a means to minimize feed costs and promote profitability of the future industry.

4. Conclusions

An analytical study of the morphology, processing attributes, fatty acid, and amino acid composition in cooked leg meat and raw hepatopancreas of juvenile male red king crabs was carried out after 12 months of live holding. Except for the increase in weight and carapace after molting, the diet composition, i.e., the ratio of raw shrimps to dry feed, influenced parameters analyzed, and it is clear that the diet composition affects the attributes of both the cooked leg meat and the raw hepatopancreas. In addition, the crumbling of the dry feed led to reduced nutritional conditions for the crabs, especially in groups with 80 and 100% dry feed. Despite this, similar overall growth performance was achieved for all the feeding groups. The effects of the reduced nutritive conditions became apparent after slaughtering and processing. In particular, a significant water loss of the clusters harvested from the 80 and 100% dry feed groups was observed. In the case of industrial processing, i.e., cooking and freezing of RKC clusters, controlling the diet and the nutritional condition is crucial to avoid economic loss in terms of reduced product yield.

We consider this study a prerequisite that provides a foundation to support further optimization of diet, feeding regime, utilization of marine by-products as protein sources, nutrient uptake, and development of technology for feeding and live holding of juvenile RKCs.

Funding

This study is a deliverable from the Nofima funded project "SIS Helt Konge" (no. 13618). Also, the Research Council of Norway is acknowledged for supporting the Aquafeed Technology Center, ATC, project number 245883/F50.

CRediT authorship contribution statement

Bjørn Tore Rotabakk: Visualization, Validation, Resources, Methodology, Investigation. **Sten I. Siikavuopio:** Writing – original draft, Resources, Methodology, Investigation, Funding acquisition, Conceptualization. **Dagbjørn Skipnes:** Visualization, Validation, Resources, Methodology, Investigation. **Grete Lorentzen:** Writing – review & editing, Writing – original draft, Visualization, Validation, Resources, Project administration, Methodology, Investigation, Funding acquisition, Formal analysis, Data curation, Conceptualization. **Anette Hustad:** Resources, Methodology, Investigation, Data curation. **Tor Andreas Samuelsen:** Writing – original draft, Visualization, Validation, Resources, Methodology, Formal analysis, Data curation, Conceptualization. **Federico Lian:** Visualization, Validation, Resources, Methodology,

Table 4
Amino acid composition (g/100 g of wet weight) of cooked leg meat and raw hepatopancreas (average ± standard deviation) of reference juveniles before starting the feeding (Wild 2022, n=6), reference juveniles in 2023 (Wild 2023, n=5), and after 12 months of feeding. The feeding groups include 100% shrimps (P0, n=5), 80% shrimps and 20% dry feed (P20, n=5), 50% shrimps and 50% dry feed (P50, n=5), 20% shrimps and 80% dry feed (P80, n=5), and 100% dry feed (P100, n=5).

	Wild 2022	***Wild 2023***	***Feeding groups***				
			P0	P20	P50	P80	P100
Cooked leg meat							
Hyp	<0.10	<0.10	<0.10	<0.10	<0.10	<0.10	<0.10
Ala	0.82 ± 0.03	0.89 ± 0.04	0.82 ± 0.06	0.79 ± 0.04	0.80 ± 0.05	0.84 ± 0.06	0.84 ± 0.03
Arg	1.58 ± 0.08	1.7 ± 0.07	1.48 ± 0.16	1.38 ± 0.13^{X}	1.42 ± 0.15	1.56 ± 0.13	1.64 ± 0.09
Asp	1.57 ± 0.05	1.7 ± 0.07	1.54 ± 0.09^{X}	1.50 ± 0.10^{X}	1.52 ± 0.04^{X}	1.62 ± 0.11	1.60 ± 0.10
Phe	0.68 ± 0.02	0.75 ± 0.04	0.68 ± 0.04^{X}	0.68 ± 0.03^{X}	0.67 ± 0.03^{X}	0.71 ± 0.04	0.68 ± 0.03^{X}
Glu	2.35 ± 0.08	2.56 ± 0.11	2.34 ± 0.15	2.26 ± 0.13^{X}	2.26 ± 0.18^{X}	2.46 ± 0.18	2.48 ± 0.08
Gly	1.33 ± 0.15	1.28 ± 0.04	1.02 ± 0.13$^{a\Delta X}$	0.93 ± 0.07$^{a\Delta X}$	0.94 ± 0.08$^{a\Delta X}$	1.14 ± 0.15^{ab}	1.28 ± 0.13^{b}
His	0.38 ± 0.01	0.41 ± 0.02	0.37 ± 0.03	0.37 ± 0.02	0.38 ± 0.01	0.40 ± 0.02	0.38 ± 0.01
Ile	0.75 ± 0.03	0.83 ± 0.03	0.74 ± 0.05^{X}	0.73 ± 0.04^{X}	0.72 ± 0.06^{X}	0.76 ± 0.05	0.75 ± 0.03
Leu	1.18 ± 0.04	1.34 ± 0.05	1.20 ± 0.07^{X}	1.18 ± 0.08^{X}	1.20 ± 0.10^{X}	1.26 ± 0.09	1.24 ± 0.05
Lys	1.27 ± 0.05	1.42 ± 0.08	1.26 ± 0.09^{X}	1.26 ± 0.05^{X}	1.24 ± 0.11^{X}	1.32 ± 0.11	1.34 ± 0.05
Met	0.50 ± 0.01	0.55 ± 0.02	0.53 ± 0.04	0.54 ± 0.04	0.51 ± 0.05	0.54 ± 0.04	0.53 ± 0.03
Pro	0.84 ± 0.06	0.91 ± 0.06	1.03 ± 0.11$^{\Delta}$	0.97 ± 0.08	0.96 ± 0.09	0.99 ± 0.11$^{\Delta}$	0.91 ± 0.07
Ser	0.72 ± 0.02	0.79 ± 0.04	0.69 ± 0.05^{X}	0.67 ± 0.03^{X}	0.68 ± 0.03^{X}	0.76 ± 0.05	0.71 ± 0.04^{X}
The	0.72 ± 0.02	0.81 ± 0.03	0.73 ± 0.05^{X}	0.71 ± 0.03^{X}	0.71 ± 0.04^{X}	0.75 ± 0.05	0.74 ± 0.04^{X}
Tyr	0.60 ± 0.02	0.66 ± 0.03	0.59 ± 0.05^{X}	0.60 ± 0.03	0.59 ± 0.03^{X}	0.62 ± 0.03	0.61 ± 0.03
Val	0.78 ± 0.03	0.85 ± 0.03	0.77 ± 0.06	0.76 ± 0.04^{X}	0.76 ± 0.05^{X}	0.80 ± 0.05	0.79 ± 0.03
Raw hepatopancreas							
Hyp	<0.10	0.77 ± 1.29	<0.10	<0.10	<0.10	<0.10	<0.10
Ala	0.56 ± 0.03	0.66 ± 0.05	0.60 ± 0.04	0.59 ± 0.05	0.65 ± 0.03	0.67 ± 0.05	0.66 ± 0.12
Arg	0.75 ± 0.05	0.83 ± 0.10	0.78 ± 0.06	0.73 ± 0.06	0.81 ± 0.05	0.71 ± 0.06	0.70 ± 0.10^{X}
Asp	1.02 ± 0.06	1.18 ± 0.08	1.08 ± 0.09^{a}	1.10 ± 0.11^{a}	1.22 ± 0.08^{a}	1.42 ± 0.11$^{ab\ \Delta}$	1.45 ± 0.29$^{b\Delta\ X}$
Phe	0.47 ± 0.02	0.54 ± 0.03	0.50 ± 0.05	0.51 ± 0.04	0.55 ± 0.03	0.56 ± 0.03$^{\Delta}$	0.54 ± 0.09
Glu	1.22 ± 0.08	1.36 ± 0.11	1.30 ± 0.07	1.28 ± 0.04	1.36 ± 0.05	1.44 ± 0.05$^{\Delta}$	1.42 ± 0.24$^{\Delta}$
Gly	0.68 ± 0.03	0.69 ± 0.07	0.78 ± 0.13	0.81 ± 0.09	0.89 ± 0.08$^{\Delta X}$	0.97 ± 0.09$^{\Delta X}$	1.00 ± 0.17$^{\Delta X}$
His	0.28 ± 0.02	0.33 ± 0.01	0.29 ± 0.03	0.30 ± 0.03	0.31 ± 0.02	0.33 ± 0.02	0.32 ± 0.06
Ile	0.45 ± 0.02	0.53 ± 0.04	0.49 ± 0.05	0.50 ± 0.04	0.64 ± 0.03	0.55 ± 0.04$^{\Delta}$	0.55 ± 0.10$^{\Delta}$
Leu	0.78 ± 0.03	0.89 ± 0.06	0.83 ± 0.07	0.82 ± 0.05	0.87 ± 0.05	0.89 ± 0.05	0.85 ± 0.13
Lys	0.72 ± 0.04	0.84 ± 0.06	0.77 ± 0.05	0.74 ± 0.05	0.80 ± 0.05	0.82 ± 0.05	0.82 ± 0.13
Met	0.27 ± 0.01	0.31 ± 0.03	0.30 ± 0.03	0.30 ± 0.02	0.32 ± 0.02	0.32 ± 0.02	0.31 ± 0.05
Pro	0.60 ± 0.04	0.59 ± 0.05	1.06 ± 0.15$^{\Delta X}$	0.87 ± 0.09$^{\Delta X}$	0.90 ± 0.09$^{\Delta X}$	1.06 ± 0.12$^{\Delta X}$	1.03 ± 0.22$^{\Delta X}$
Ser	0.50 ± 0.04	0.57 ± 0.04	0.53 ± 0.05	0.53 ± 0.04	0.57 ± 0.03	0.61 ± 0.05	0.59 ± 0.11
The	0.53 ± 0.02	0.63 ± 0.04	0.57 ± 0.06	0.58 ± 0.04	0.62 ± 0.04	0.64 ± 0.05	0.62 ± 0.11
Tyr	0.42 ± 0.02	0.48 ± 0.04	0.46 ± 0.05	0.46 ± 0.05	0.50 ± 0.03	0.53 ± 0.05$^{\Delta}$	0.51 ± 0.10
Val	0.56 ± 0.02	0.66 ± 0.05	0.61 ± 0.07	0.61 ± 0.05	0.66 ± 0.04	0.68 ± 0.05$^{\Delta}$	0.68 ± 0.12$^{\Delta}$

Note. Results are expressed as mean values (± standard deviation). Different superscript letters within the same row of the fed RKCs indicate significantly different mean values ($p < 0.05$, full factorial ANOVA followed by Scheffe's test). Furthermore, Δ and X indicate significant differences between the fed RKCs and the wild RKCs from 2022 and 2023, respectively. ($p < 0.05$).
Abbreviations: Hyp, hydroksyproline; Ala, alanine; Arg, arginine; Asp, aspartic acid; Phe, phenylalanine; Glu, glutamat acid; Gly, glycine; His, histidine; Ile, isoleucine; Leu, leucine; Lys, lysine; Met, methionine; Pro, proline; Ser, serine; The, threonine; Tyr, tyrosine; Val, valine

Investigation, Conceptualization. **Tina Thesslund:** Resources, Methodology, Investigation, Data curation.

Declaration of Competing Interest

The authors declare that they have no known competing financial interests or personal relationships that could have appeared to influence the work reported in this paper.

Data Availability

Data will be made available on request.

Acknowledgements

The authors are grateful to colleagues at Nofima's Feed Technology Centre, employees at the Nofima BioLab laboratory (Bergen, Norway), and Tromsø for technical support.

Appendix A. Supporting information

Supplementary data associated with this article can be found in the online version at doi:10.1016/j.jfca.2024.106310.

References

Albalat, A., Johnson, L., Coates, C.J., Dykes, G.C., Hitte, F., Morro, B., Dick, J., Todd, K., Neil, D.M., 2019. The Effect of Temperature on the Physiological Condition and Immune-Capacity of European Lobsters (*Homarus gammarus*) During Long-Term Starvation. Front. Mar. Sci. 6 https://doi.org/10.3389/fmars.2019.00281.

Barrento, S., Marques, A., Teixeira, B., Anacleto, P., Vaz-Pires, P., Nunes, M.L., 2009. Effect of Season on the Chemical Composition and Nutritional Quality of the Edible Crab *Cancer pagurus*. J. Agric. Food Chem. 57 (22), 10814–10824. https://doi.org/10.1021/jf9025597.

Bell, J.W., Farkas, B.E., Hale, S.A., Lanier, T.C., 2001. Effect of Thermal Treatment on Moisture Transport during Steam Cooking of Skipjack Tuna (*Katsuwonas pelamis*). In: Journal of Food Science, 66. Portico, pp. 307–313. https://doi.org/10.1111/j.1365-2621.2001.tb11337.x.

Bligh, E.G., Dyer, W.J., 1959. A rapid method of total lipid extraction and purification. Can. J. Biochem. Physiol. 37 (8), 911–917. https://doi.org/10.1139/o59-099.

Blikra, M.J., Skipnes, D., Feyissa, A.H., 2019. Model for heat and mass transport during cooking of cod loin in a convection oven. Food Control 102, 29–37. https://doi.org/10.1016/j.foodcont.2019.03.001.

Bogevik, A.S., Samuelsen, T.A., Aspevik, T., Romarheim, O.H., Aas, T.S., Kalananthan, T., Rønnestad, I., 2021. Disintegration stability of extruded fish feed affects gastric functions in Atlantic salmon (Salmo salar). Aquaculture 543, 737006. https://doi.org/10.1016/j.aquaculture.2021.737006.

Borisov, R.R., Epelbaum, A.B., Kryakhova, N.V., Tertitskaya, A.G., Kovatcheva, N.P., 2007. Cannibalistic behavior in red king crabs reared under artificial conditions. Russ. J. Mar. Biol. 33 (4), 227–231. https://doi.org/10.1134/s1063074007040049.

Cervellione, F., McGurk, C., Van den Broeck, W., 2017. Perigastric organ": a replacement name for the "hepatopancreas" of Decapoda. J. Crustace Biol. 37 (3), 353–355. https://doi.org/10.1093/jcbiol/rux020.

Christiansen, J.S., Sparboe, M., Sæther, B., Siikavuopio, S.I., 2015. Thermal behaviour and the prospect spread of an invasive benthic top predator onto the Euro-Arctic shelves. In: Diversity and Distributions, 21. Portico, pp. 1004–1013. https://doi.org/10.1111/ddi.12321.

Cohen, S.A., Michaud, D.P., 1993. Synthesis of a Fluorescent Derivatizing Reagent, 6-Aminoquinolyl-N-Hydroxysuccinimidyl Carbamate, and Its Application for the Analysis of Hydrolysate Amino Acids via High-Performance Liquid Chromatography. Anal. Biochem. 211 (2), 279–287. https://doi.org/10.1006/abio.1993.1270.

Conradi-Larsen, T., Lian, F., Hustad, A., Siikavuopio, S.I., Vang, B., 2024. Use of whole and processed lumpfish as feed for red king crab (*Paralithodes camtschaticus*) during three-month live holding. prep.

Cunningham, D.T., 1969. A study of the food and feeding relationships of the Alaskan king crab, *Paralithodes camtschaticus*. MS thesis, San Diego State College, San Diego, CA.

D'Abramo, L.R., Conklin, D.E., Akiyama, D.M., 1997. Crustace Nutr. J. World Aquacult Soc. vol. 6.

Dima, J.B., Barón, P.J., Zaritzky, N.E., 2012. Mathematical modeling of the heat transfer process and protein denaturation during the thermal treatment of Patagonian marine crabs. J. Food Eng. 113 (4), 623–634. https://doi.org/10.1016/j.jfoodeng.2012.07.007.

Dooley, P.C., Crouch, P.J., West, J.M., 2002. Free amino acids in claw muscle and haemolymph from Australian freshwater crayfish at different stages of the moult cycle. Comp. Biochem. Physiol. Part A: Mol. amp; Integr. Physiol. 131 (3), 625–637. https://doi.org/10.1016/s1095-6433(01)00487-1.

Dvoretsky, A.G., Bichkaeva, F.A., Baranova, N.F., Dvoretsky, V.G., 2020. Fatty Acid Composition in the Hepatopancreas of the Barents Sea Red King Crab. Biol. Bull. 47 (4), 332–338. https://doi.org/10.1134/s1062359020040044.

Gibson, R., Barker, P.L., 1979. The decapod hepatopancreas. Ann. Rev. vol. 17, 285–346.

Hartnoll, R.G., 1982. Growth. In: Bliss, D. (Ed.), The biology of Crustacea. Academic Press, New York, pp. 111–196.

Huang, S., Wang, L.M., Sivendiran, T., Bohrer, B.M., 2017. Review: Amino acid concentration of high protein food products and an overview of the current methods used to determine protein quality. Crit. Rev. Food Sci. Nutr. 58 (15), 2673–2678. https://doi.org/10.1080/10408398.2017.1396202.

ISO 5983-2, 2009. Animal feeding stuffs. Determination of nitrogen content and calculation of crude protein content. Part 2: Block digestion and steam distillation method. International Organization for Standardization. Geneva, Switzerland. https://doi.org/10.3403/3312294u.

ISO 5984, 2022. Animal feeding stuffs. Determination of crude ash. International Organization for Standardization. Geneva, Switzerland. https://doi.org/10.3403/30400911.

ISO 6496, 1999. International Organization for Standardization. Animal feeding stuffs. Determination of moisture and other volatile matter content. Geneva, Switzerland.

James, P., Vasilyev, R., Siikavuopio, S., Kovatcheva, N., Samuelsen, T.A., Mundheim, H., Carlehög, M., 2013. The effects of varying the percentage of herring versus salmon protein in manufactured diets on the survival, meat content, hepatosomatic index and meat sensory quality of adult red king crab *Paralithodes camtschaticus* held in captivity. Aquaculture 416–417, 390–395. https://doi.org/10.1016/j.aquaculture.2013.08.002.

Jewett, S.C., Feder, H.M., 1982. Food and feeding habits of the king crab *Paralithodes camtschatica* near Kodiak Island, Alaska. Mar. Biol. 66 (3), 243–250. https://doi.org/10.1007/bf00397029.

Jewett, S.C., Gardner, L.A., Rusanowski, P.M., 1990. Food and feeding habits of red king crab from north-western Norton Sound, Alaska. In: Melteff, C.B. (Ed.), International King and Tanner Crab Symposium. University of Alaska Sea Grant Program, Anchorage, AK, pp. 219–232.

Kattner, G., Graeve, M., Calcagno, J.A., Lovrich, G.A., Thatje, S., Anger, K., 2003. Lipid, fatty acid and protein utilization during lecithotrophic larval development of *Lithodes santolla* (Molina) and *Paralomis granulosa* (Jacquinot). J. Exp. Mar. Biol. Ecol. 292 (1), 61–74. https://doi.org/10.1016/s0022-0981(03)00143-6.

Kousoulaki, K., Mørkøre, T., Nengas, I., Berge, R.K., Sweetman, J., 2016. Microalgae and organic minerals enhance lipid retention efficiency and fillet quality in Atlantic salmon (*Salmo salar* L.). Aquaculture 451, 47–57. https://doi.org/10.1016/j.aquaculture.2015.08.027.

Li, X., Han, T., Zheng, S., Wu, G., 2021. Nutrition and Functions of Amino Acids in Aquatic Crustaceans. Amino Acids Nutr. Health 169–198. https://doi.org/10.1007/978-3-030-54462-1_9.

Lian, F., Lorentzen, G., Siikavuopio, S.I., 2019. Live holding of red king crab (*Paralithodes camtschaticus*) – Effect of time, temperature, and feeding on quality of processed clusters, 7-9 November, 2019 Presentation at ICES Shellfish symposium. Tromsø, Norway.

Lian, F., Siikavuopio, S.I., Harrison, S.M., Vang, B., Brunton, N.P., Esaiassen, M., Lorentzen, G., 2022. Fatty acid composition of cooked leg meat and raw hepatopancreas of red king crab (*Paralithodes camtschaticus*) during three-month live holding without feeding at 5 and 10 °C. J. Food Compos. Anal. 105, 104206 https://doi.org/10.1016/j.jfca.2021.104206.

Lian, F., Siikavuopio, S.I., Hustad, A., Thesslund, T., Lindberg, S.-K., Lorentzen, G., 2021. Comparative quality evaluation of processed clusters obtained from red king crab (*Paralithodes camtschaticus*) typical of spring and autumn harvests in the Barents Sea (Article). Food Control 123, 107826. https://doi.org/10.1016/j.foodcont.2020.107826.

Liu, X., Zhao, J., Zheng, Y., Sun, N., Li, X., Yang, R., 2018. Genetic Analysis for Absolute and Relative Growth of Body Weight and Main Morphological Traits in Chinese Mitten Crab (*Eriocheir sinensis*). In: Journal of the World Aquaculture Society, 49. Portico, pp. 380–387. https://doi.org/10.1111/jwas.12518.

Lorentzen, G., Lian, F., Siikavuopio, S.I., 2019. Quality parameters of processed clusters of red king crab (*Paralithodes camtschaticus*) - Effects of live holding at 5 and 10 °C up to 92 days without feeding. Food Control 95, 142–149. https://doi.org/10.1016/j.foodcont.2018.07.041.

Lorentzen, G., Lian, F., Hustad, A., Thesslund, T., Esaiassen, M., Siikavuopio, S.I., 2023. Evaluation of Morphological and Quality Parameters in Adult Male Red King Crabs (*Paralithodes camtschaticus*) Raised to Commercial Weight from Juveniles. Aquacult. Res. 2023, 1–11. https://doi.org/10.1155/2023/6884272.

Lorentzen, G., Voldnes, G., Whitaker, R.D., Kvalvik, I., Vang, B., Gjerp Solstad, R., Thomassen, M.R., Siikavuopio, S.I., 2018. Current Status of the Red King Crab (*Paralithodes camtchaticus*) and Snow Crab (*Chionoecetes opilio*) Industries in Norway. Rev. Fish. Sci. Aquacult. 26 (1), 42–54. https://doi.org/10.1080/23308249.2017.1335284.

McLeod, L.E., Carter, C.G., Johnston, D.J., 2004. Changes in the body composition of adult male southern rock lobster, *Jasus edwardsii*, during starvation. J. Shellfish Res. 23, 257–264.

Mente, E., Deguara, S., Santos, M.B., Houlihan, D., 2003. White muscle free amino acid concentrations following feeding a maize gluten dietary protein in Atlantic salmon (*Salmo salar* L.). Aquaculture 225, 133–147. https://doi.org/10.1016/S0044-8486(03)00285-0.

Mizuta, S., Kobayashi, Y., Yoshinaka, R., 2001. Chemical and Histological Characterization of Raw Muscle from Soft and Hard Crabs of Snow Crab *Chionoecetes opilio*. In: Journal of Food Science, 66. Portico, pp. 238–241. https://doi.org/10.1111/j.1365-2621.2001.tb11324.x.

Nguyen, N.T.B., Chim, L., Lemaire, P., Wantiez, L., 2014. Feed intake, molt frequency, tissue growth, feed efficiency and energy budget during a molt cycle of mud crab juveniles, Scylla serrata (Forskål, 1775), fed on different practical diets with graded levels of soy protein concentrate as main source of protein. Aquaculture 434, 499–509. https://doi.org/10.1016/j.aquaculture.2014.09.014.

Norwegian Ministry of Fisheries and Coastal Affairs, 2007. Stortingsmelding nummer 40 (2006–2007). Forvaltning Av. kongekrabbe. [Manag. Red. king crab. Report to the Parliament no. 40 (2006–2007)]. https://www.regjeringen.no/no/dokumenter/stmeld-nr-40-2006-2007-/id480559/?ch=2 (accessed the 21nd of February 2024). (In Norwegian).

NRC, 2011. Nutrient requirements of fish and shrimp. The National Academies Press, Washington, DC.

Powell, G.C., 1967. Growth of the King Crabs in the Vicinity of Kodiak Island, Alaska. Alaska Department of Fish and Game Informational Leaflet. Alaska Department of Fish and Game, Kodiak, AK.

Råfisklaget, 2024. https://www.rafisklaget.no/ <Accessed the 2nd of March 2024>

Risso, S.J., Carelli, A.A., 2012. Nutrient Composition of Raw and Cooked Meat of Male Southern King Crab (*Lithodes santolla Molina*, 1782). J. Aquat. Food Prod. Technol. 21 (5), 433–444. https://doi.org/10.1080/10498850.2011.608482.

Rosa, R., Nunes, M.L., 2003. Nutritional quality of red shrimp, *Aristeus antennatus* (Risso), pink shrimp, *Parapenaeus longirostris* (Lucas), and Norway lobster, *Nephrops norvegicus* (Linnaeus). In: Journal of the Science of Food and Agriculture, 84. Portico., pp. 89–94. https://doi.org/10.1002/jsfa.1619

Saborowski, R., 2015. Physiology, The natural history of the crustacea. In: Chang, E.S., Thiel, M. (Eds.), Nutrition and Digestion. Oxford University Press, NY, US, pp. 285–319.

Sacristán, H.J., Rodríguez, Y.E., De los Angeles Pereira, N., López Greco, L.S., Lovrich, G. A., Fernández Gimenez, A.V., 2017. Energy reserves mobilization: Strategies of three decapod species. PLOS ONE 12 (9), e0184060. https://doi.org/10.1371/journal.pone.0184060.

Samuelsen, T.A., Haustveit, G., Kousoulaki, K., 2022. The use of tunicate (*Ciona intestinalis*) as a sustainable protein source in fish feed – effects on the extrusion process, microstructure, and physical pellet properties. Anim. Feed Sci. Technol. 284, 115193 https://doi.org/10.1016/j.anifeedsci.2021.115193.

Siikavuopio, S.I., Aksnes, A., Hope, B., Kristoffersen, K., Dale, T., Carlehög, M. (2006). Utvikling av spesialfôr til kongekrabbe (Paralithodes camtschaticus). Fiskeriforskning Rapport 1/2006. In norwegian.

Siikavuopio, S.I., James, P., Olsen, B.R., Evensen, T., Mortensen, A., 2014. Holding wild caught red king crab, *Paralithodes camtschaticus*: effects of stocking density and feeding on survival and meat content. In: Aquaculture Research, 47. Portico., pp. 870–874. https://doi.org/10.1111/are.12546

Siikavuopio, S.I., James, P., 2013. Effects of temperature on feed intake, growth and oxygen consumption in adult male king crab *Paralithodes camtschaticus* held in captivity and fed manufactured diets. Aquac. Res. 46 (3), 602–608. https://doi.org/10.1111/are.12207.

Siikavuopio, S.I., Martinsen, G., Stenberg, E., Jakobsen, R., Carlehög, M., Eilertsen, G., 2011. Kongekrabbe – foredling Og. Ind. bearbeiding. Report no. 6/2011. In norwegian.

Sikora, M., Złotek, U., Kordowska-Wiater, M., Świeca, M., 2021. Spicy Herb Extracts as a Potential Improver of the Antioxidant Properties and Inhibitor of Enzymatic Browning and Endogenous Microbiota Growth in Stored Mung Bean Sprouts. Antioxidants 10 (3), 425. https://doi.org/10.3390/antiox10030425.

Simon, C.J., 2009. Digestive enzyme response to natural and formulated diets in cultured juvenile spiny lobster, *Jasus edwardsii*. Aquaculture 294 (3–4), 271–281. https://doi.org/10.1016/j.aquaculture.2009.06.023.

Skipnes. D. (2011). Optimisation of thermal processing of fresh farmed cod. Philosophiae Doctor (PhD) Thesis. Dept. of Mathematical Sciences and Technology, Norwegian University of life science, Ås, Norway. https://nmbu.brage.unit.no/nmbu-xmlui/bitstream/handle/11250/2434097/2011-17_Dagbj%c3%b8rn%20Skipnes_%28IMT%29.pdf?sequence=1&isAllowed=y.

Skipnes, D., Van der Plancken, I., Van Loey, A., Hendrickx, M.E., 2008. Kinetics of heat denaturation of proteins from farmed Atlantic cod (Gadus morhua). J. Food Eng. 85 (1), 51–58. https://doi.org/10.1016/j.jfoodeng.2007.06.030.

Sundet, J.H., Hoel, A.H., 2016. The Norwegian management of an introduced species: the Arctic red king crab fishery. Mar. Policy 72, 278–284. https://doi.org/10.1016/j.marpol.2016.04.041.

Torstensen, B.E., Lie, Ø., Frøyland, L., 2000. Lipid metabolism and tissue composition in Atlantic salmon (*Salmo salar* L.)—effects of capelin oil, palm oil, and oleic acid-enriched sunflower oil as dietary lipid sources. Lipids 35, 653–664. https://doi.org/10.1007/s11745-000-0570-6.

Vilasoa-Martínez, M., López-Hernández, J., Lage-Yusty, M.A., 2007. Protein and amino acid contents in the crab, *Chionoecetes opilio*. Food Chem. 103 (4), 1330–1336. https://doi.org/10.1016/j.foodchem.2006.10.045.

Wen, X., Chen, L., Ku, Y., Zhou, K., 2006. Effect of feeding and lack of food on the growth, gross biochemical and fatty acid composition of juvenile crab, *Eriocheir sinensis*. Aquaculture 252 (2–4), 598–607. https://doi.org/10.1016/j.aquaculture.2005.07.027.